University of California, San Diego
Department of Structural Engineering
Structural Systems Research Project

Report No. SSRP- 99/18

Design Example of a Multiple Column Bridge Bent Under Seismic Loads Using the Alaska Cast-In-Place Steel Shell

by

Pedro F. Silva
Post-Doctoral Research Engineer

Frieder Seible
Professor of Structural Engineering

Final Report to Alaska Department of Transportation
and Public Facilities, Juneau, Alaska, under Project Number 53205

Department of Structural Engineering
University of California, San Diego
La Jolla, California 92093-0085

October 1999

Technical Report Documentation Page

1. Report No.	2. Government Accession No.	3. Recipient's Catalog No.
SSRP 99/18		

4. Title and Subtitle	5. Report Date
Design Example of a Multiple Column Bridge Bent Under Seismic Loads Using the Alaska Cast-in-Place Steel Shell	February 1999
	6. Performing Organization Code

7. Author(s)	8. Performing Organization Report No.
P. F. Silva, F. Seible	UCSD SSRP-99/8

9. Performing Organization Name and Address	10. Work Unit No. (TRAIS)
Division of Structural Engineering School of Engineering University of California, San Diego La Jolla, California 92093-0085	11. Contract or Grant No. 53205

12. Sponsoring Agency Name and Address	13. Type of Report and Period Covered
Federal Highway Administration Alaska Department of Transportation and Public Facilities 3132 Channel Drive Juneau, Alaska, 99801-78989	Final 14. Sponsoring Agency Code

15. Supplementary Notes

Prepared in cooperation with the State of Alaska Department of Transportation and Public Facilities.

16. Abstract

Consistent with the principles of a capacity design philosophy, the ideal approach for the seismic design of reinforced concrete multiple column bridge bents is to conveniently select plastic hinges to form in the top and bottom of columns. As plastic hinges develop in the top and bottom of columns, inspection and repair can be achieved without significant traffic disruption, and a ductile performance is easily achieved by the confining action of steel shells and/or transverse reinforcement. Thus, the earthquake energy is dissipated in the column plastic hinge through hysteretic damping. In addition, cap beams are protected from any significant inelastic actions, as these members are not conveniently used to provide energy dissipation.

Using these principles of seismic design a design example was prepared, which was based on the Knik River Overflow Bridge, situated north of Anchorage. Analytical results based on a pushover and time history seismic assessment indicate that the cap beam design is adequate in ensuring a ductile performance, and plastic hinges will form at the top of the pile shaft/columns.

17. Key Words	18. Distribution Statement
concrete, seismic design, bridges, columns, pile shafts pile cap connections, joint design	Unlimited

19. Security Classification (of this report)	20. Security Classification (of this page)	21. No. of Pages	22. Price
Unclassified	Unclassified	44	

Disclaimer

Opinions, findings, conclusions and recommendations expressed in this design example are those of the authors and do not necessarily reflect views of the Federal Highway Administration and the State of Alaska Department of Transportation and Public Facilities.

Acknowledgments

The research project described in this report was funded by the Federal Highway Administration and the State of Alaska Department of Transportation and Public Facilities under project No. 53205.

We greatly appreciate the input and coordination provided by Mr. Richard Pratt and Mr. Elmer Marx from the Alaska Department of Transportation and Public Facilities during the development of this design example.

List of Symbols

A_b Cross sectional area of a reinforcing bar.

A_g Gross sectional area of concrete section.

A_{sl} Total longitudinal steel area.

A_{shell} Cross sectional area of the steel shell.

b_j Effective joint width.

c Section neutral axis.

C_c Concrete compression force.

C_s' Reinforcing steel compression force.

C_{shell} Steel shell compression force.

D Column diameter or width.

D_j Steel shell outside diameter.

D_i Steel shell inside diameter.

d_b Diameter of reinforcement bar.

E_c Young's modulus of concrete or initial tangent modulus of elasticity of concrete.

E_s Young's modulus of reinforcing steel.

E_{sec} Secant modulus of elasticity of concrete.

E_{shell} Young's modulus of steel shell.

f_c' Concrete compressive strength.

f_h Horizontal axial stress in the joint region.

f_v Vertical axial stress in the joint region.

f_y Yield strength of steel reinforcement.

f_{yj} Yield strength of steel shell.

f_y^o Reinforcement yield strength at overstrength.

I_{eff} Effective moment of inertia.

h_b Depth of pier cap.

h_{cur} Height of curvature cell.

l_d Development length of reinforcing steel.

M_C Column moment.

P_C Column axial load.

P_h Horizontal axial force on the joint.

P_v Vertical axial force on the joint.

T_s Reinforcing steel tension force.

T_{shell} Steel shell tension force.

t_j Steel shell thickness.

V_C Column shear force.

V_{jv} Vertical joint shear force.

v_{jv} Vertical joint shear stress.

Δ Lateral deflection.

Δ_y Yield displacement.

Δ_U Ultimate displacement.

μ_Δ Displacement ductility.

ρ_t Joint principal tensile stress.

ρ_{sj} Volumetric ratio of the steel shell.

φ Section curvature.

Table of Contents

ABSTRACT

Consistent with the principles of a capacity design philosophy, the ideal approach for the seismic design of reinforced concrete multiple column bridge bents is to conveniently select plastic hinges to form in the top and bottom of columns. As plastic hinges develop in the top and bottom of columns, inspection and repair can be achieved without significant traffic disruption, and a ductile performance is easily achieved by the confining action of steel shells and/or transverse reinforcement. Thus, the earthquake energy is dissipated in the column plastic hinge through hysteretic damping. In addition, cap beams are protected from any significant inelastic actions, as these members are not conveniently used to provide energy dissipation.

Using these principles of seismic design a design example was prepared, which was based on the Knik River Overflow Bridge, situated north of Anchorage. Analytical results based on a pushover and time history seismic assessment indicate that the cap beam design is adequate in ensuring a ductile performance, and plastic hinges will form at the top of the pile shaft/columns.

1 Introduction

A detailed list of recommendations for the design of Multiple Column Bridge Bents is described in reference [1]. This research project was developed for the State of Alaska department of transportation and public facilities to provide guidelines for the seismic design of multiple column bridge bents constructed with cast in place steel shells. In order to illustrate the implementation of these recommendations, a design example was prepared and is presented in this report. In this design example the Knik River Overflow Bridge, which is situated north of Anchorage, was selected as the prototype structure.

Ten bridge structures built in the State of Alaska were assessed for seismic response using models developed at the University of California San Diego. Analyses of these bridges under simulated seismic loads indicated that there is a high propensity for excessive damage to these bridges. Analysis findings are presented in **Tables 1-1** through **1-3**.

As illustrated in these tables some of the design deficiencies identified were:

(i) Excessive Amounts of Column Longitudinal Reinforcement. For example, a column with a longitudinal reinforcement ratio as high as 9% was identified in the columns of the Susitna River Bridge (see **Table 1-1**). This high level of reinforcement ratio imposes very large shear demands in the joints and consequently, requires impracticable amounts of reinforcement in the joints.

(ii) Potential for Plastic Hinging in the Cap Beam. In **Table 1-2** the Chena River Bridge cap beam yield flexural strength to column ideal flexural strength ratio of approximately 45% was identified. Consequently, inadequate longitudinal reinforcement in the cap beam will not prevent inelastic actions from developing in these members under seismic loading.

(iii) Inadequate Joint Shear Reinforcement. Most of the bridges presented in **Table 1-3** indicate inadequate joint shear reinforcement to resist undesirable inelastic actions in the connection of the beam to the column.

(iv) Deficient Cap Beam Shear Strength. Inadequate transverse reinforcement was also identified in some of these bridges, as described in **Table 1-3**. Inadequate confinement of plastic hinges in the cap beam will result in brittle shear failure of the cap beam.

(v) Embedment of Steel Shells in the Joint Region. A pile shaft/column, commonly employed in the construction of bridges in the State of Alaska, consists of a cast-in-place steel shell section (CISS), which is embedded into the cap beam/column connection. Even at low levels of column rotation, damage to the cap beam bottom surface cover concrete would be inevitable due to the prying action of the embedded portion of the steel shell. This may result in exposure of the cap beam reinforcement to corrosive environments and premature corrosion of this reinforcement, which would be potentially hazardous under seismic actions.

Table 1-1 State of Alaska Bridge Sections – Column Section Design Parameters

Bridge Section	Column Diameter in. (mm)	Shell Thickness in. (mm)	Column Longitudinal Reinforc.	Shell Ratio % A sh / A g	Reinforc. Ratio % A st / Ac
MATANUSKA	48 (1220)	1 (25.40)	32 - #11	8.2	2.8
EAST FORK	24 (610)	1 (25.40)	-	16.0	-
KNIK	48 (1220)	1 (25.40)	19 - #18	8.2	4.2
CHENA	42 (1067)	3/4(19.05)	56 - #10	7.0	5.1
CANYON	36 (914)	1 (25.40)	12 - #11	11.0	1.8
SHIP	36 (914)	1/2 (12.70)	32 - #10	5.5	4.0
KLUTINA	36 (914)	1 (25.40)	12 - #9	11.0	1.2
GEIST	30 (762)	1/2 (12.70)	20 - #9	6.5	2.8
SUSITNA	24 (610)	3/4 (19.05)	32 - #10	12.1	9.0
KNIK	36 (914)	3/4 (19.05)	12 - #10	8.2	2.0
MULTI-COLUMN TEST	36 (914)	1/2 (12.70)	16 - #11	5.5	2.5

Table 1-2 State of Alaska Bridge Sections - Cap Beam Section Design Parameters

Bridge Section	Cap Beam Width in. (mm)	Cap Beam Depth in. (mm)	Cap Beam Longit. Reinforc.	Reinforc. Ratio % A s / Ac	Vertical Stirrups within Hb
MATANUSKA	72 (1829)	60 (720)	10 - #11	0.40	10 - #5
EAST FORK	48 (1220)	30 (762)	10 - #11	1.25	40 - #5
KNIK	72 (1829)	60 (720)	10 - #11	0.40	12 - #6
CHENA	60 (720)	42 (1070)	10 - #10	0.55	8 - #5
CANYON	54 (1372)	33 (838)	10 - #9	0.65	24 - #5
SHIP	48 (1220)	48 (1220)	14 - #9	0.66	12 - #6
KLUTINA	54 (1372)	48 (1220)	8 - #9 8 - #10	0.35	10 - #5
GEIST	60 (720)	36 (914)	7 - #10	0.45	12 - #6
SUSITNA	45 (1143)	42 (1067)	8 - #9	0.47	16 - #6
KNIK	54 (1372)	36 (914)	6 - #9	0.35	8-#6
MULTI-COLUMN TEST	54 (1370)	42 (1070)	10 - #9 13 - #9	0.50	42 - #4

Table 1-3 State of Alaska Bridge Sections - Expected Failure Mode

Bridge Section	$\frac{My,cap}{Mi,col}$ %	$\frac{V_{capacity}}{V_{design}}$ %	Joint P t $\sqrt{f'c}$	$\frac{A\ v}{A\ jv}$ %	EXPECTED FAILURE MODE
MATANUSKA	70	96*	5.5	35	Cap Beam Flexure Joint Shear
EAST FORK	90	290*	15	95	Cap Beam Flexure Joint Shear
KNIK	50	70*	8	40	Cap Beam Flexure Joint Shear
CHENA	45	99*	14	20	Cap Beam Flexure Joint Shear
CANYON	70	620*	7.5	230	Cap Beam Flexure
SHIP	84	340*	7	75	Cap Beam Flexure Joint Shear
KLUTINA	140	170	3	110	Ductile Response
GEIST	80	175*	6.5	140	Cap Beam Flexure
SUSITNA	70	275*	10.5	110	Cap Beam Flexure
KNIK	50	332	5	120	Cap Beam Flexure
MULTI-COLUMN TEST	105	112	7	105	Ductile Response

In order to address the above design deficiencies and to ensure a proper ductile response of multiple column bridge bents, findings from recent research studies at UCSD were used to design the Alaska Cast-In-Place Steel Shell Three Column Bridge Bent test unit. Experimental results were then used to validate the design recommendations developed for the seismic design of reinforced concrete bridge bents with cast-in-place steel shells.

Design recommendations were developed in accordance with the capacity design philosophy and were as follows:

(i) Column Longitudinal Reinforcement. In reference **[2]**, the recommended upper limit for the column steel ratio is 4%, and ratios below 3% are normally found in the design of bridge columns. Consequently, the longitudinal reinforcement ratio was limited to 2.5% consistent with the design recommendations by Priestley et al.**[2]**.

(ii) Anchorage of Column Longitudinal Reinforcement. In order to improve constructability of the joint regions, the column longitudinal bars were terminated straight into the cap beam.

(iii) Steel Shell Embedment. In order to protect the cap beam from extensive damage due to the prying action of the steel shells, the steel shells were terminated 2in. (51mm) below the cap beam.

(iv) Confinement of Plastic Hinges. Confinement of the column plastic hinge at the gap region was ensured by providing adequate transverse reinforcement to constrain buckling of the column longitudinal reinforcement and permit large inelastic rotations.

(v) Cap Beam Design. Design of the cap beam was developed in order to ensure an elastic response of this member under any seismic action that imposes the overstrength moment in the columns.

(vi) Joint Design. Design of the connection between the cap beam and the columns was performed to achieve joint constructability and to limit significant damage within the joint region under seismic actions.

Competence of the design procedure established for reinforced concrete bridge bents was examined in a proof test by studying the influence of the design issues described above on the overall seismic response of the full-scale test unit as presented in [1]. Based on the seismic performance of the test unit, appropriate design recommendations were made, and in a parallel analytical study an attempt was made to present a design example that illustrates the implementation of these design procedures.

Following an introduction to the design deficiencies, which are presented in **Tables 1-1** through **1-3**, found in some of the bridges built in the State Alaska and a list of the design details presented in reference [1], **Chapter 2** describes the current Knik River Overflow Bridge structure. The expected failure mode of the prototype structure was determined based on a pushover analysis and time history analysis. **Chapter 3** presents the redesign of this bridge based on the recommended design procedure. Finally, this design example report concludes with specific recommendations for the seismic design of reinforced concrete bridge bents with cast-in-place steel shell pile-shaft/columns, as presented in **Chapter 4** and outlined in more detail in reference [1].

2 Seismic Assessment of the Knik River Overflow Bridge

Application of the design recommendations presented in reference [1] will be illustrated for a typical multiple column bridge bent in the form of a design example. The bridge selected for this design example was the Knik River Overflow Bridge, which is a two span bridge with a center four pile/column bridge bent, as shown schematically in **Figure 2-1**.

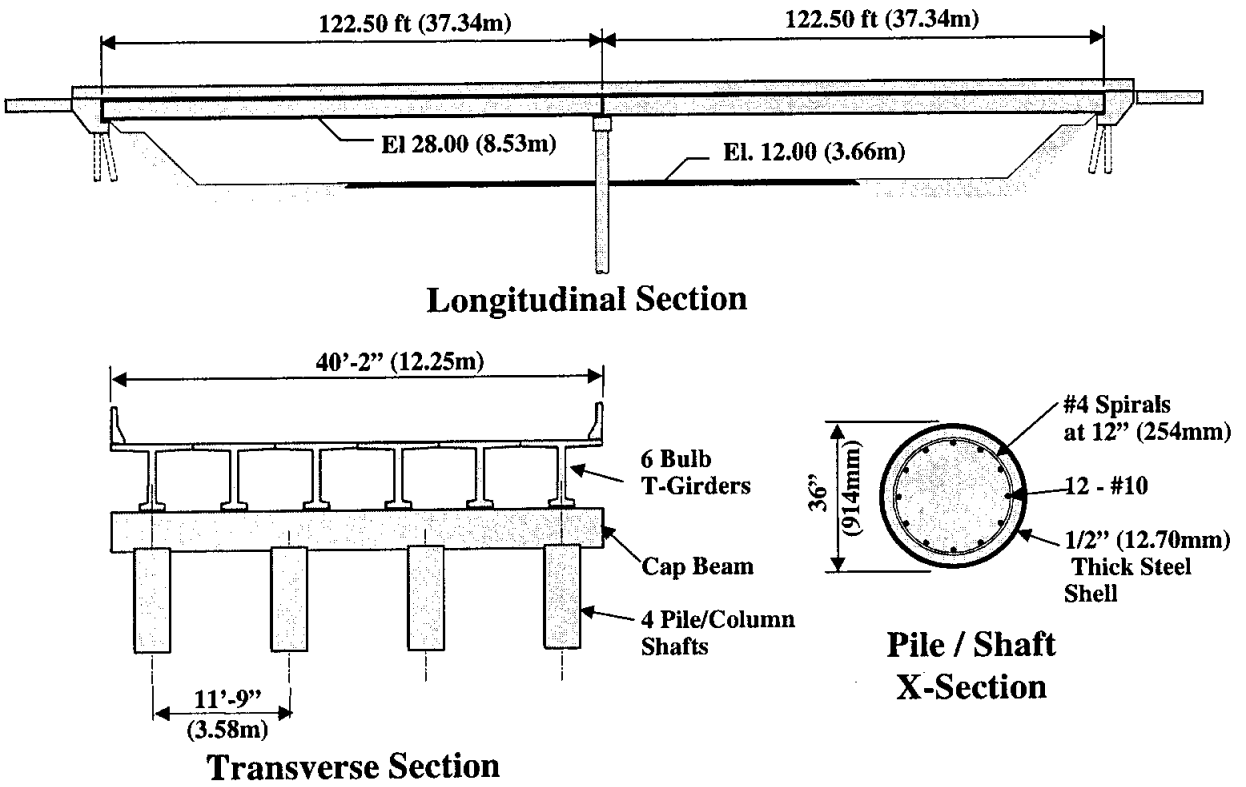

Figure 2-1 Knik River Overflow Bridge - Prototype Structure

For this bridge, the pile shaft/columns consist of a cast in place steel shell with an inside diameter of 36in. (914 mm) embedded 2in. (50.80mm) into the cap beam, and a shell thickness of 1/2in. (12.70mm), as shown in **Figure 2-1** and **Figure 2-2**. The connection to the cap beam consists of 12-#10 bent bars for a longitudinal reinforcement ratio of 2%.The transverse reinforcement consists of #6 bars at a spiral pitch of 3 in. (76.20 mm) in the top 60in. (1.52 m), and #6 bars at a spiral pitch of 12in. (305 mm) below this region. The cap beam dimensions are 54 in (1.37 m) wide by 36 in. (914 mm) deep, reinforced with 6-#9 bars in the top and bottom layer of reinforcement and 2-#9 bars on either side. The transverse reinforcement consists of #6-2 legged stirrups at 10 in. (254 mm) on centers.

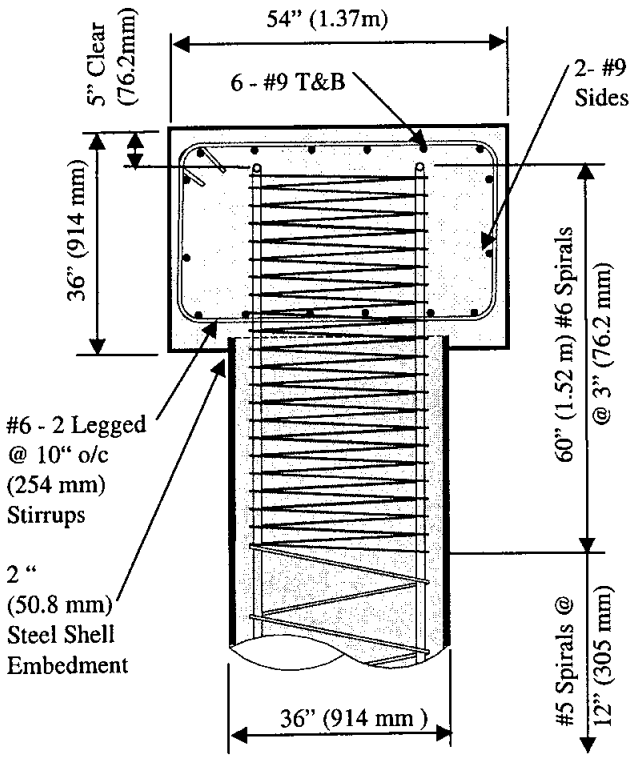

Figure 2-2 Column/Cap Beam Joint Section

2.1 Material Properties

Concrete and steel material properties used in the analysis of the prototype and redesign structure presented in **Chapters 2** and **3**, respectively, are presented in Table 2-1

Table 2-1 Material Properties

	Longitudinal Reinforcement		Longitudinal Reinforcement		
	f_y ksi [Mpa]	f_U ksi [Mpa]	f_y ksi [Mpa]	Spacing in. [mm]	Concrete Strength
COLUMN	66 [455]	99 [683]	66 [455]	3 [76.20]	5 [35]
CAP BEAM	60 [414]	60 [414]	60 [414]	10 [254]	3 [21]

2.2 Pushover Analysis Response

In this section, a brief description of the pushover analysis response is presented. The pushover analysis in this study was conducted through a control program, which interacted with a moment-curvature analysis program and a finite element structural analysis program, as presented in reference **[1]**. The soil-structure interaction analysis was performed using the discrete finite element model illustrated in **Figure 2-3**. Some of the parameters that had to be considered in this model were the bending stiffness of the pile shaft/columns and cap beam, and the axial stiffness of the soil, both in the vertical and horizontal direction.

2.2.1 Modeling of the Prototype Structure

Critical issues in the modeling of the pile shaft/columns were the composite action between the steel shell and concrete core in the connection and subgrade regions, embedment of the steel shell into the cap beam and confinement of the concrete core by the steel shells. The influence of these design parameters in the load deformation response of CISS sections were experimentally and analytically studied in a test program conducted at UCSD, as presented in reference **[3]**, and are extensive detailed in reference **[1]**.

In addition, the soil was modeled as an array of uncoupled linear elastic spring elements. Elements to model the soil were only placed on one side of the pile, because the axial stiffness of the members to represent the soil stratum were the same in compression and in tension. In this work, the analytical subgrade reaction model, typically known as the Winkler model, was used for the analysis under simulated seismic loading. In the Winkler model, the soil strength is characterized by the relation between soil pressure and displacement by the coefficient of subgrade reaction as described in **Figure 2-3**. A great advantage in modeling the soil by uncoupled, discrete springs, is the ease of obtaining a solution using any structural program that uses discrete truss and beam elements.

Additional issues related to the iteration procedure are beyond the scope of work described in this report, and may be found in references **[1]** and **[3]**.

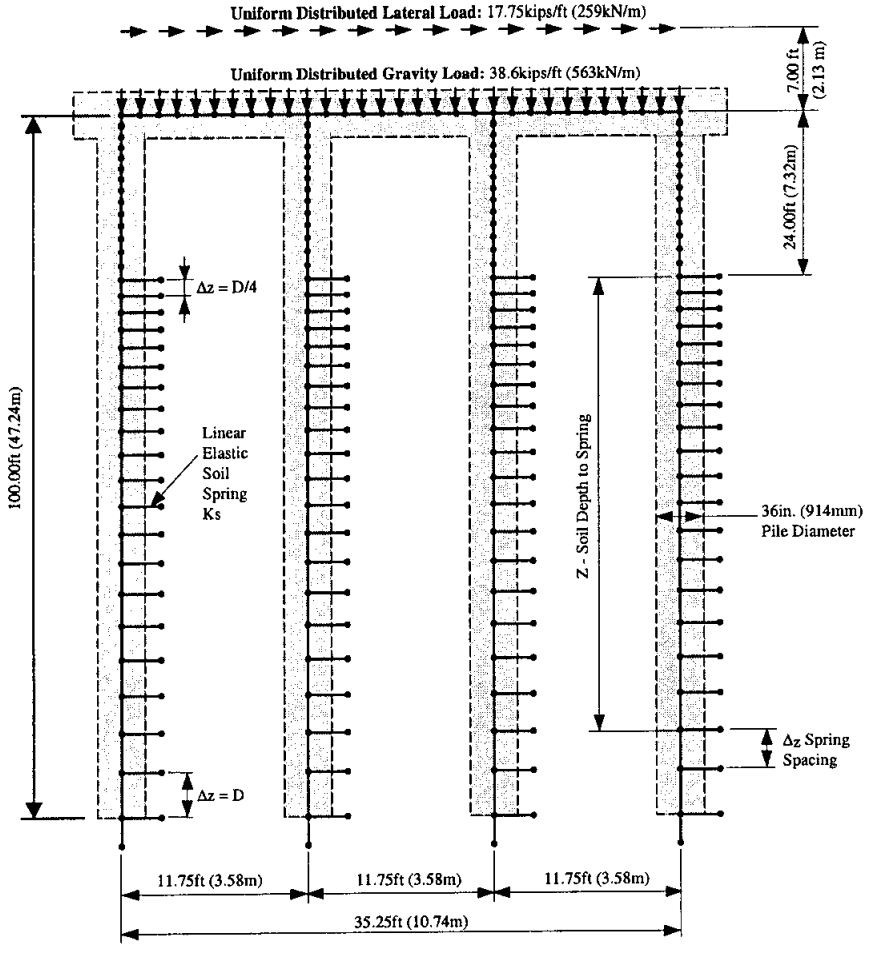

Figure 2-3 Soil-Structure Interaction Finite Element Model

2.2.2 Pushover Analysis Results

The pushover analysis lateral force-deformation relationships and limit states are plotted in **Figure 2-4**. Limit states at critical events are also plotted in **Figure 2-4** from cracking of the cap beams, to joint shear failure and full formation of the plastic mechanism.

Limit states presented in **Figure 2-4** indicate that failure occurs due to the limited capacity either of the cap beam or joints. This pushover analysis predicts that large tensile strains in the cap beam longitudinal reinforcement and compressive strains in the concrete core will be achieved, which impose large rotational demands in the cap beams. Because of limited amounts of transverse reinforcement in the cap beam plastic hinge regions, it is expected that premature buckling of the cap beam longitudinal reinforcement and shear failure will occur without achieving the flexural capacity

either of the cap beam or columns. In addition, insufficient joint shear reinforcement will most likely lead to failure in the joint regions.

Also presented in **Figure 2-4** are the spectral forces and displacement obtained from the time history, which will be presented in the next section. According to the spectral displacement the structure will not be capable of resisting the imposed deformations. Thus, even if proper detailing for the transverse and joint shear reinforcement is provided, failure of the structure is expected to occur due to fracture of the longitudinal reinforcement. A detailed explanation of the time history analysis is presented in the next section.

Cap beam and column moment curvature relationships are presented in **Figure 2-5**. Columns will be subjected to minimum curvature ductility demands, but the cap beam will be subjected to large curvature ductility demands, as previously described.

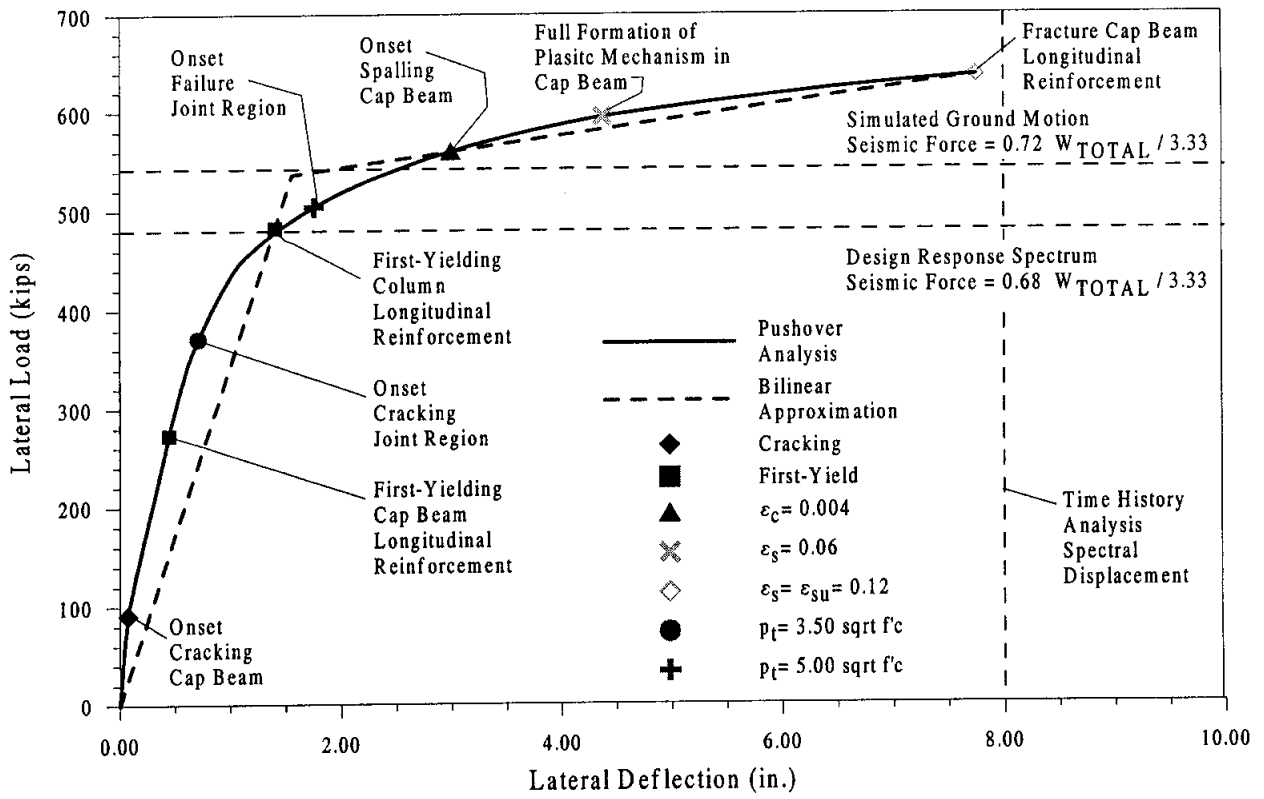

Figure 2-4 Lateral Force-Deformation and Limit States From Pushover Analysis

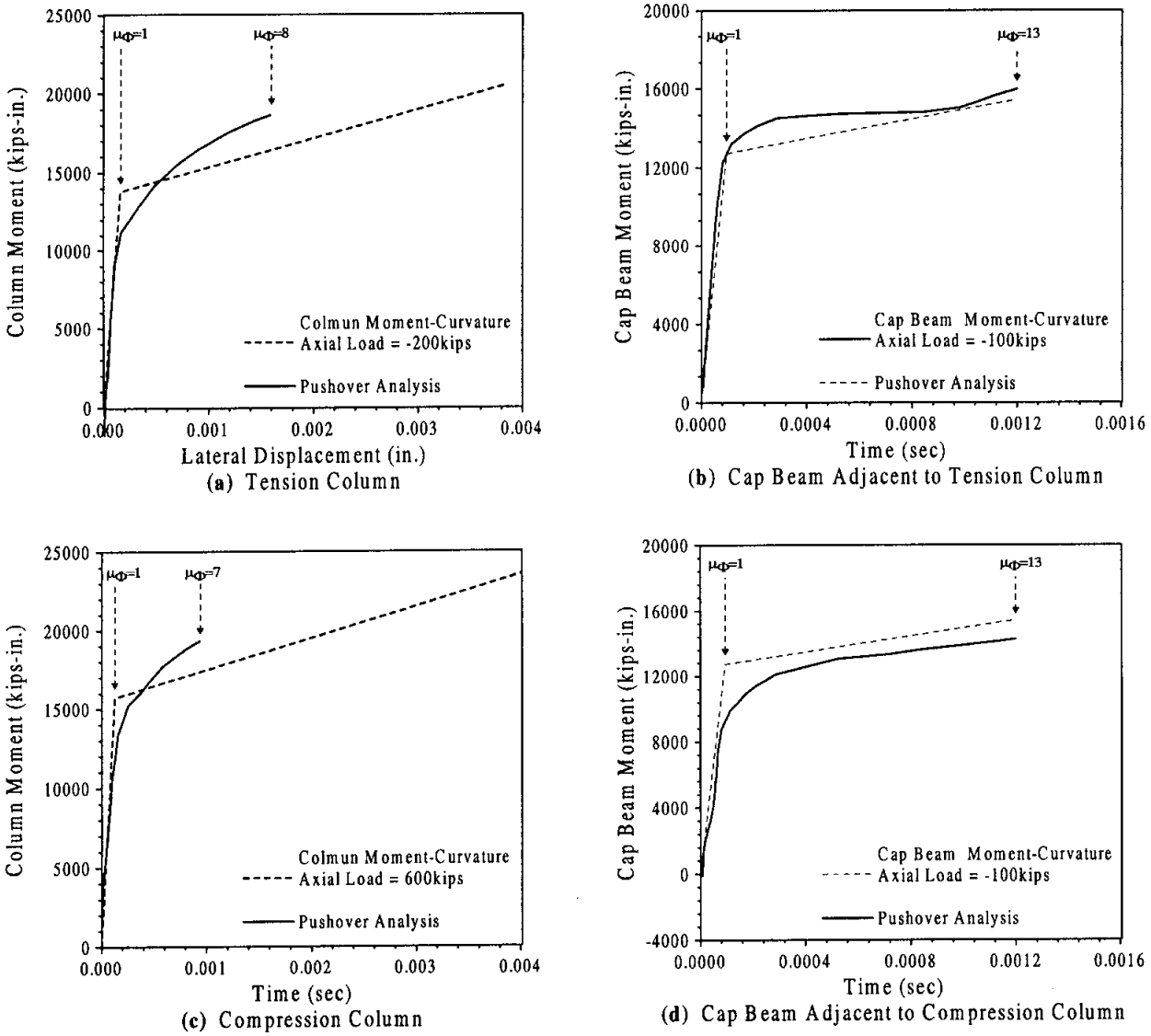

Figure 2-5 Pile Shafts/Columns and Cap Beam Moment-Curvature Relationships From Pushover Analysis

2.3 Time History Analysis Response

In this section, analysis of the section was performed using a time history simulated ground motion, which spectrum approximates the design spectrum, as presented in **Figure 2-6**. The design spectrum was the typical AASHTO design spectrum obtained according to the expression [4]:

$$\frac{1.2\,A\,S}{T_N^{2/5}} \leq 2.50\,A \qquad (2.1)$$

where A is the a peak ground acceleration, S is the site soil profile coefficient, and T_N is the natural

period of the bridge. Design values for this particular bridge were; A=0.40g and S=1.5, which corresponds to soil Type III. The bridge natural period was estimated at 1.10sec, which will be presented in the next section.

To reduce the complexity of the time history analysis the columns were modeled as cantilever members to the point of contra-flexure in the subgrade region, as depicted in **Figure 2-7(b)**.

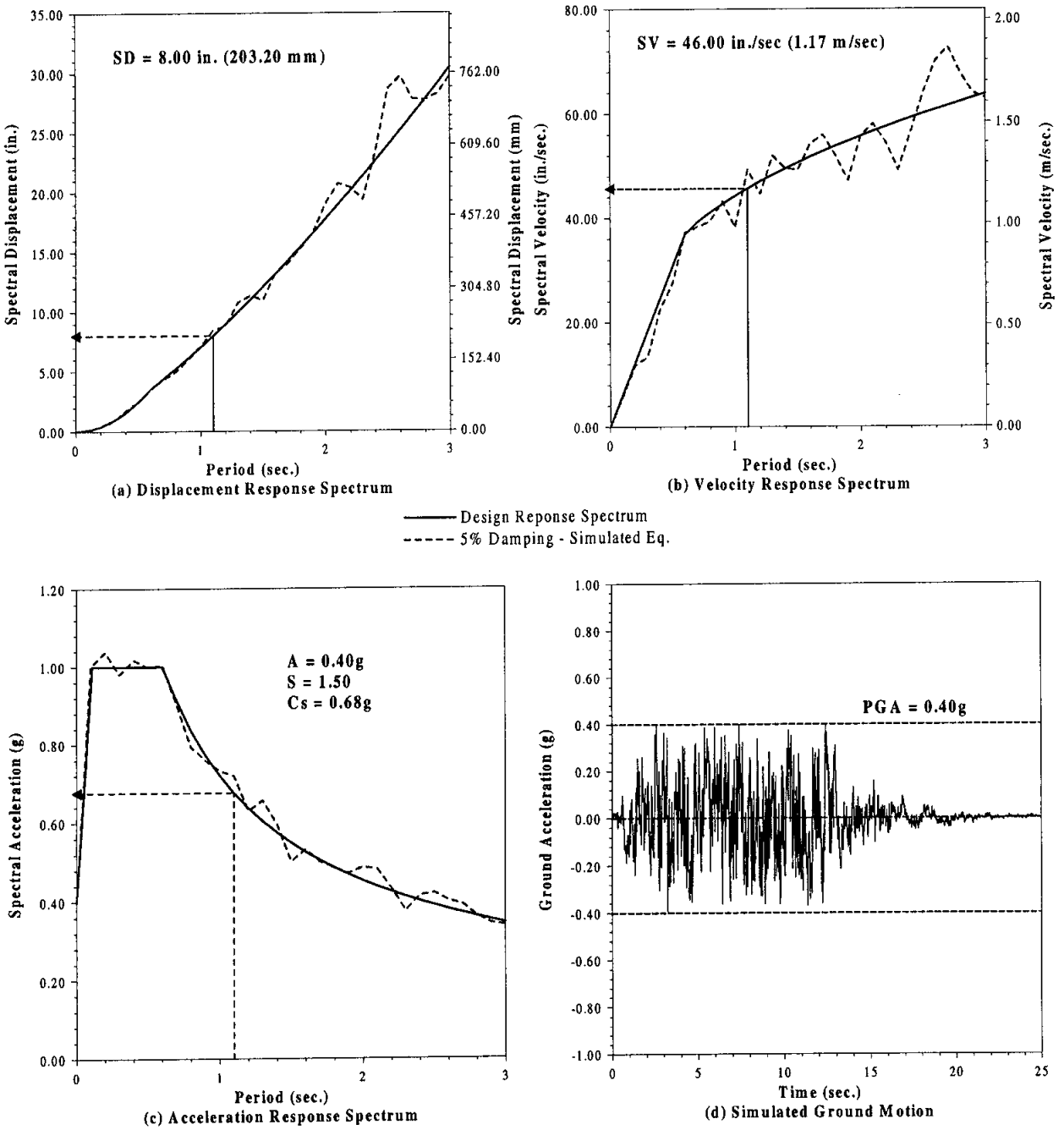

Figure 2-6 Simulated Ground Motion and Design Response Spectrum

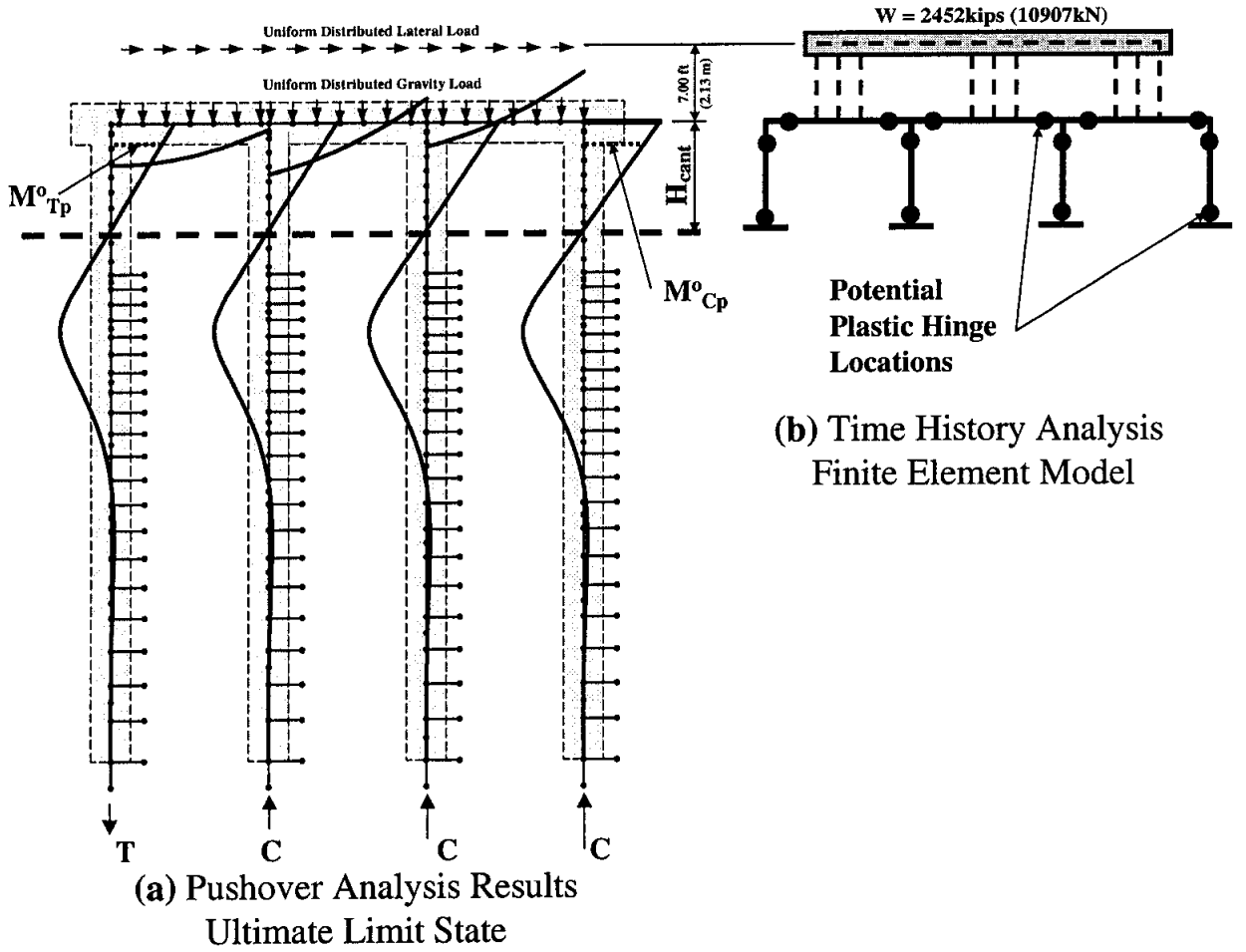

Figure 2-7 Soil-Structure Interaction Finite Element Model for the Time History Analysis

2.3.1 Effective Cantilever Length and Structure Natural Period

The columns effective cantilever length used in the finite element model for the time history analysis were obtained from curves developed by Budek et al [2], which illustrates the depth to fixity concept. Thus, in a similar analysis it is not necessary to run a pushover analysis, but one may directly compute the effective cantilever length by employing these or similar curves.

In order to estimate the effective cantilever length the coefficient of horizontal subgrade reaction, k_h, used in this analysis was 40 kips/ft^3 (6279 kN/m^3). The effective bending stiffness, EI_{eff}, of the columns was obtained from a bilinear approximation, as depicted in **Figure 2-8**.

Based on the values for the coefficient of horizontal subgrade reaction, k_h, effective bending stiffness, EI_{eff}, column diameter, D, and effective column diameter of 6ft (1.83m), D^*, the soil/structure stiffness parameter was obtained according to the expression [2]:

$$\frac{1000\ K\ D^6}{D^*\ EI_{eff}} = \frac{1000\ x\ 40\ x\ 3\ x\ 3^6}{6\ x\ 1.13x10^6} = 13.00 \qquad (2.1)$$

Plotting the soil/structure stiffness parameter in **Figure 2-9** the columns effective cantilever length, H_{cant}, used in the time history analysis was 12.75ft (3.89m).

The elastic period of the structure, T_N, was estimated at 1.10 sec, which was computed according to the Rayleigh's Method. Calculations to estimate T_N are presented in **Table 2-2**. Referring back to **Figure 2-7**, the distance from the cap beam center line to the center line of the superstructure center of mass was estimated at 7.00ft (2.13m).

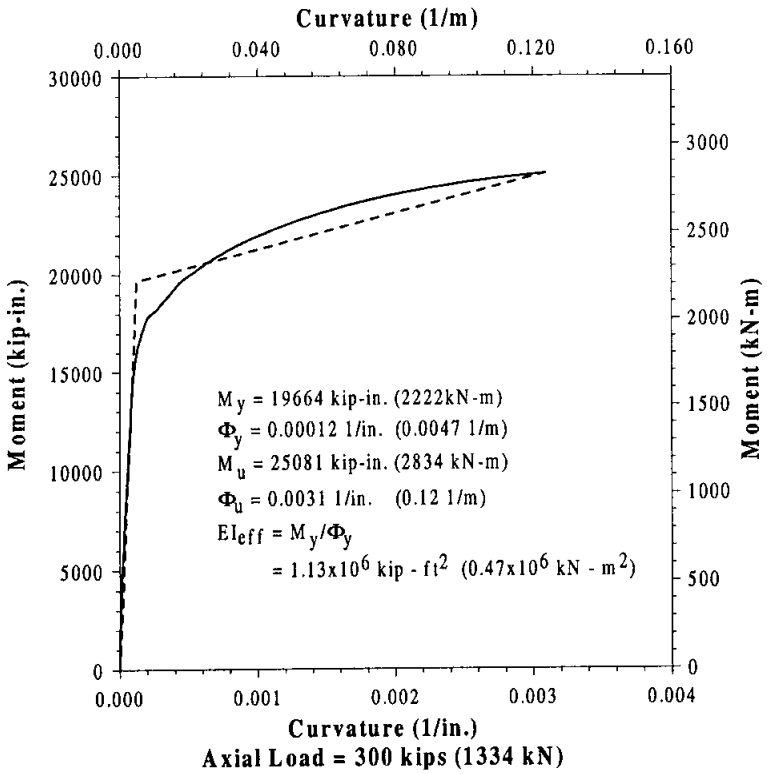

Figure 2-8 Steel Shell Encased Reinforced Concrete Column, Axial Load P=300 kips

Elastic Stiffness

$$K_{eff} = \frac{3\,EI_{eff}}{H_{eff}^{3}} = 1636 \text{ kips / ft} \quad (24024 \text{ kN/m})$$

$$K^{*}_{eff} = \frac{3\,EI_{eff}}{H^{*3}_{eff}} = 440 \text{ kips / ft} \quad (6464 \text{ kN/m})$$

$$H^{*}_{eff} = 12.75 + 3 + 4 \text{ ft} = 19.75 \text{ ft (6.02m)}$$

Soil-Structure Stiffness Parameters

$k_h = 40$ kips/ ft^3 (6279 kN / m^3)

$k = Dk_h = 120$ kips/ ft^2 (5746 kN/ m^2)

$1000\,k\,D^6 / (D^*\,EI_{eff}) \approx 13.00$

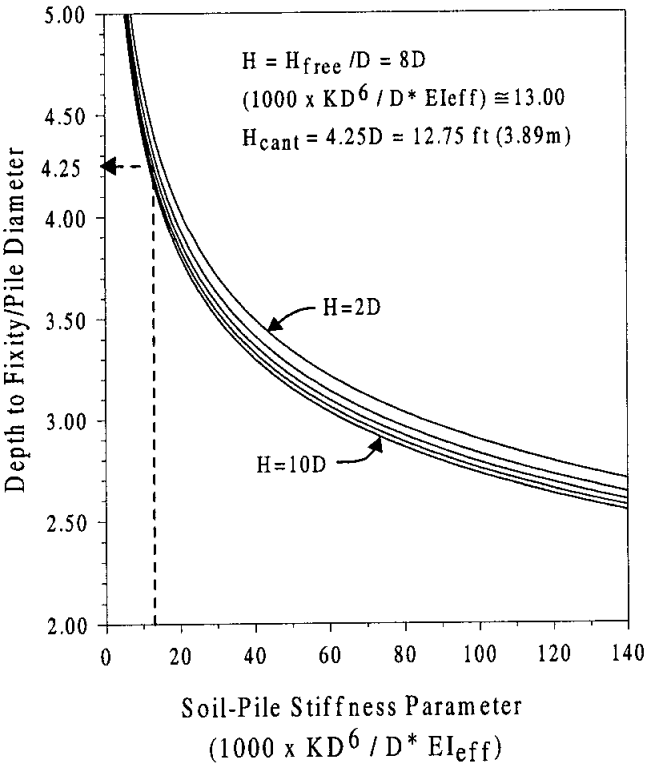

Figure 2-9 Computation of Column Effective Cantilever Length After Budek **[3]**

Table 2-2 Natural Period - Rayleigh's Method

Member	W kips (kN)	K kips / ft (kN / m)	L ft (m)	ϕi	$\Delta\phi i$	$W\phi i^2$	$K\Delta\phi i^2$
Superstructure	2452 (10907)	1760 (25856)	19.75 (6.02)	1.00	0.42	2452 (10907)	310 (4561)
Column + Cap Beam	112 (498)	6544 (96096)	14.25 (4.34)	0.58	0.58	38 (168)	2202 (32327)
					Cantilevered Column, T = 1.10 sec	2489 (11061)	2512 (36888)

2.3.2 Time History Analysis Results

An elastic and nonlinear time history analyses were performed using the simulated ground motion presented in **Figure 2-6(d)**, and the finite element model described in **Figure 2-6(b)**. The modified Takeda model was the model used to characterize the hysteretic behavior of the columns and cap beam. This model was based on the bilinear approximation presented in **Figures 2-8** and **2-10** for the columns and cap beam, respectively.

Elastic and nonlinear moments at the top of the columns located on the extreme sides and the adjacent cap beam moments are plotted in **Figures 2-11(a)** and **2-11(b)**, respectively. Calculations for force reduction factors are presented in **Table 2-3**, which indicate that a force reduction factor, ***R***, of approximately 3.47 will be achieved. In addition in **Figures 2-11(c)** and **2-11(d)** are presented the column top displacement for the elastic and nonlinear analysis, respectively. Values presented in **Table 2-4** indicate that a displacement ductility, μ_Δ, of approximately 3.90 will be achieved. This value is approximately the same as the ***R*** value, which characterizes the equal-displacement principle established for an inelastic system [2]. The calculated displacement ductility is slight below the recommended value of μ_Δ=4.00, which was based on observations recorded during testing [1]. Thus, a slight reduction in the moment capacity of the columns may be implemented in the redesign of this structure, which will be one of the objectives in **Chapter 3**.

In **Figures 2-12(a)** and **2-12(b)** are presented the columns and cap beam moment-curvature relationships, respectively, obtained from the nonlinear time history analysis. Referring to **Figure 2-12(a)**, it is clear that the columns under the imposed seismic actions will be subjected to minor inelastic deformations. However, large inelastic rotations will be imposed on the cap beam, as illustrated in **Figure 2-12(b)** and previously demonstrated while presenting the pushover analysis results. Thus, the cap beams must be redesigned in order to achieve a proper ductile response of the structure, which is another objective that will be presented in **Chapter 3**.

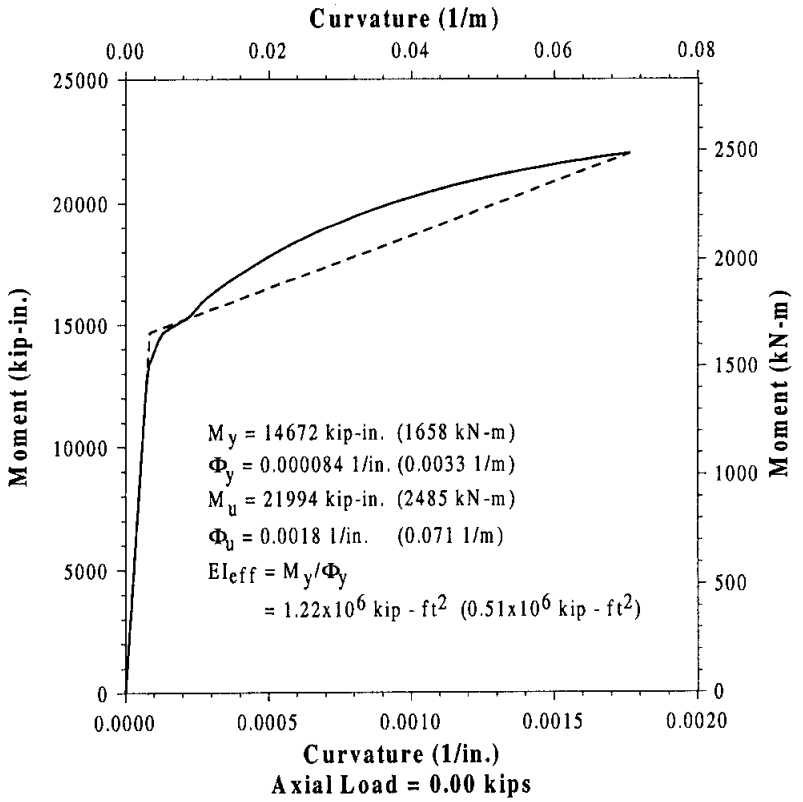

Figure 2-10 Cap Beam, Axial Load P = 0 kips

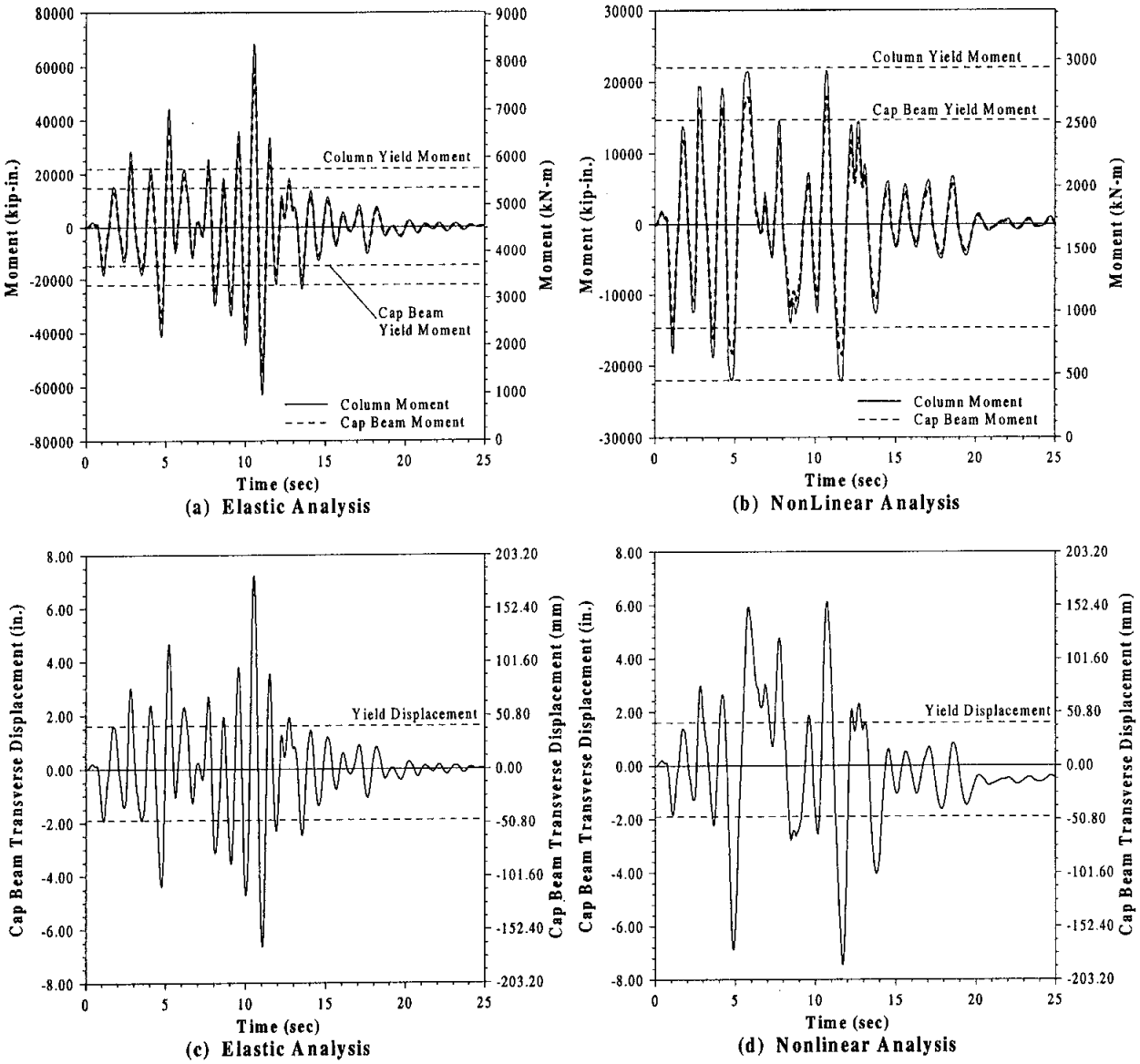

Figure 2-11 Simulated Ground Motion Lateral Force and Displacement From Time History Linear and Nonlinear Analysis

Table 2-3 Force Reduction Calculations
From Time History Analysis

	W_{TOTAL} kips (kN)	V_E kips (kN)	Cs g	V_D kips (kN)	R V_E / V_D
Bridge Weight	2600 (11565)	1872 (8327)	0.72	540 (2402)	3.47

Table 2-4 Displacement Ductility Calculations
From Time History Analysis

	Δ_y in. (mm)	Δ_d in. (mm)	$\mu\Delta_d$
Column Top Displacement	1.90 (48.26)	7.40 (188.00)	3.90

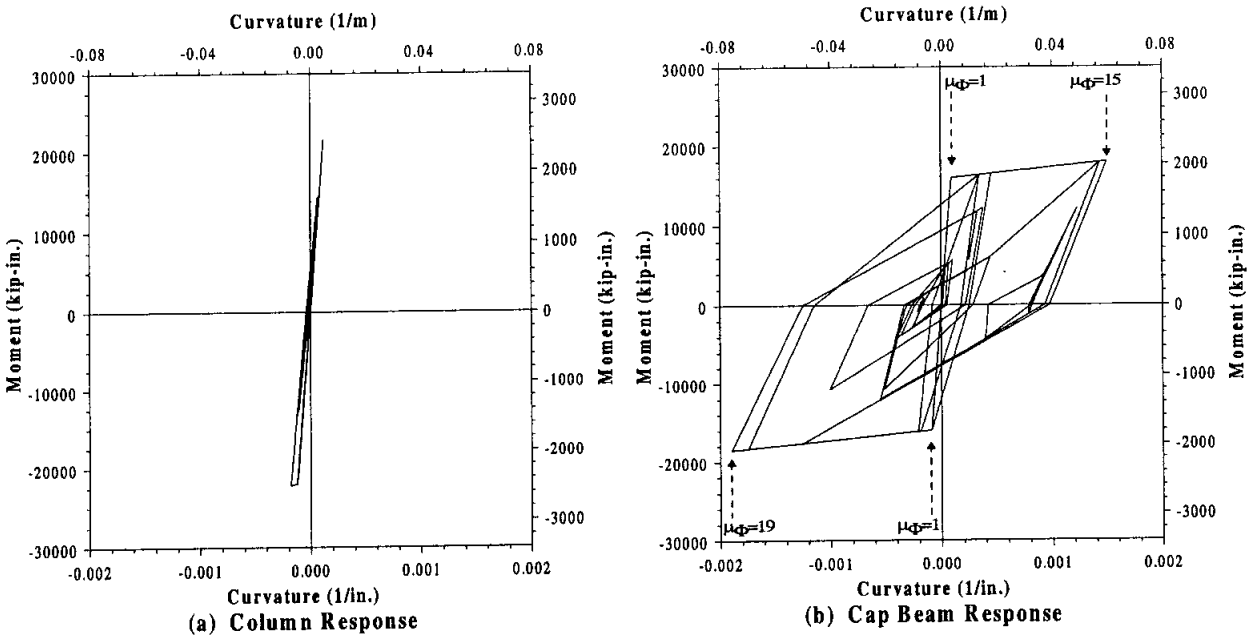

Figure 2-12 Moment vs. Curvature Relationships
From Time History Nonlinear Analysis

3 Seismic Redesign of the Knik River Overflow Bridge Bent

Seismic assessment of the Knik River Overflow Bridge, as presented in **Chapter 2**, has proven the likelihood for failure of this bridge below the design level. Deficiencies, which were encountered in the design of this bridge, have shown that under a seismic event below the design earthquake level the following failure modes are expected: (1) cap beam flexural failure, (2) cap beam shear failure, and (3) joint shear failure. In this chapter redesign of the Knik River Overflow Bridge is developed based on the design procedure presented in reference **[1]**.

The main design issues that were addressed in the redesign of this bridge bent were as follows:

(i) *Column Longitudinal Reinforcement* was designed according to the design response spectrum previously described and a force reduction factor, ***R***, of **4**. The design was then checked to ensure that the displacement ductility did not exceed **4**.

(ii) *Anchorage of the Column Longitudinal Reinforcement* was satisfied by designing the cap beam with the appropriate depth for adequate development of the pile shaft/column longitudinal reinforcement.

(iii) *Steel Shell Embedment* into the cap beam was not adopted. Instead, a steel shell gap of 2in (50.80mm) below the cap beam is proposed to ensure that overstrength moments and damage to the cap beam, due to the prying action of the steel shell, do not occur.

(iv) *Confinement of Plastic Hinges* at the top of the pile shaft/columns was provided to ensure that buckling of the column longitudinal reinforcement and shear failure do not occur in the gap region.

(v) *Cap Beam Flexural and Shear Design* was performed to ensure that plastic hinges only developed at the top of the pile shaft/columns.

(vi) *Joint Design* was performed according to joint shear force transfer mechanisms, as described in reference **[1]**, to ensure the proper formation of plastic hinge at the at the top of the pile shaft/columns.

3.1 Preliminary Seismic Design

Design of the Knik River Overflow Bridge was developed to satisfy the design issues previously described. Assuming the natural period, T_N, of 1.10sec and an effective cantilever length of 12.75m (3.89m) for the columns, as described in **Chapter 2**, the preliminary design moment calculations for the pile shaft/columns are presented in **Table 3-1**.

Table 3-1 Preliminary Design Moment Calculations

Member	W kips (kN)	Cs g	V_E kips (kN)	V_D/Col kips (kN)	L ft (m)	M_D/Col kips-in. (kN-m)
Superstructure	2452 (10907)	0.68	1667 (7417)	104.25 (464)	12.75 (3.89)	15950 (1802)
Column + Cap Beam	112 (498)	0.68	76 (338)	5 (22)	12.75 (3.89)	765 (86)
				Design Moment for Individual Columns =		16715 (1889)

Based on **Table 3-1** the design moment for the individual pile shaft/columns was 16,715kips-in. (1889kN-m). A moment curvature analysis for the section described in **Figure 3-1** was performed for an axial load of 340kips (1512kN),which represents approximately the average axial load present in the columns. The X-section presented in **Figure 3-1(b)** is identical to the prototype section, but the steel shell is not embedded into the cap beam, as shown in **Figure 3-1(a)**. The force equilibrium equations used to develop the moment curvature analysis are described in reference **[1]**. In establishing the force equilibrium calculations a transverse reinforcement with a spacing of 1in (25.4mm) is proposed in the gap region.

Since, the average ideal capacity of this section was 17900kips-in. (2022kN-m), as described in **Figure 3-2**, which is slightly higher than the required moment capacity, this section was then used for the design of the bridge bent. Complete design of the bridge bent is presented in the next section.

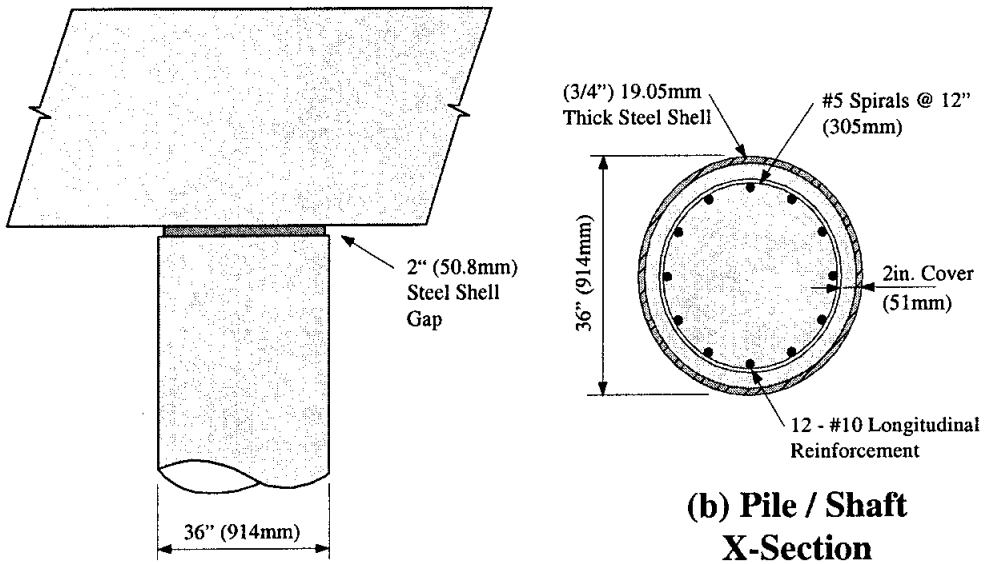

(a) Cap Beam/Joint Elevation

(b) Pile / Shaft X-Section

Figure 3-1 Pile Shaft / Column X-Section

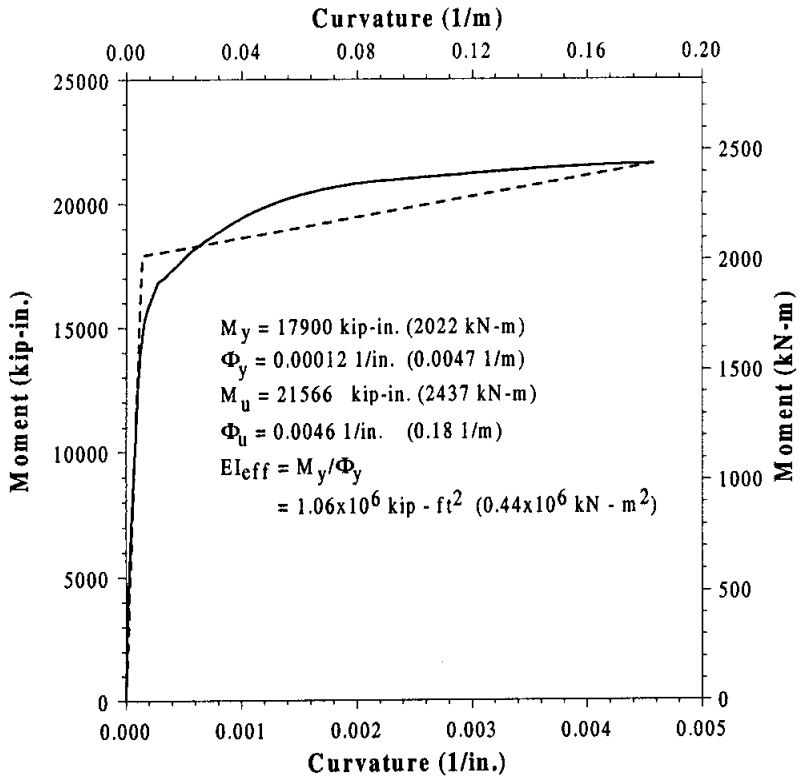

Transverse Reinforcement
Size = #5
Spacing = 1in. (25.40mm)

Axial Load = 340kips (1512kN)

Figure 3-2 Reinforced Concrete Section for the Column Gap Region

3.2 Bridge Bent Seismic Design

Seismic design was performed using the AASHTO design spectrum previously described in **Eq. (2.1)**. The response spectrum design values were the same presented in **Chapter 2**, which were: A=0.40g and S=1.5, which corresponds to soil Type III. The bridge bent natural period was 1.07sec, which will be presented in the next section. As before, the columns effective cantilever length were obtained from curves developed by Budek et al [2]. In this analysis, the coefficient of horizontal subgrade reaction, k_h, was 40 kips/ft^3 (6279 kN/m^3). The effective bending stiffness, EI_{eff}, of the columns was obtained from a bilinear approximation of the moment curvature analysis presented in **Figure 3-2**.

Based on the values for the coefficient of horizontal subgrade reaction, k_h, effective bending stiffness, EI_{eff}, column diameter, D, and effective column diameter of 6ft (1.83m), D^*, the soil/structure stiffness parameter was obtained according to the expression [2]:

$$\frac{1000\,K\,D^6}{D^*\,EI_{eff}} = \frac{1000 \times 40 \times 3 \times 3^6}{6 \times 1.06 \times 10^6} \approx 13.75 \qquad (3.1)$$

Plotting the soil/structure stiffness parameter value of 13.75 in **Figure 3-3** the columns effective cantilever length, H_{cant}, used in the time history analysis was 12.00ft (3.66m).

Elastic Stiffness

$K_{eff} = \frac{3\,EI_{eff}}{H_{eff}^3} = 1840$ kips / ft (26852 kN/m)

$K^*_{eff} = \frac{3\,EI_{eff}}{H^*_{eff}{}^3} = 464$ kips / ft (6772 kN/m)

$H^*_{eff} = 12.00 + 3 + 4$ ft
$= 19.00$ ft (5.80 m)

Soil-Pile Stiffness Parameters

$k_h = 40$ kips/ ft^3 (6279 kips/ ft^3)
$k = Dk_h = 120$ kips/ ft^2 (5746 kN/ m^2)
$1000\,k\,D^6 / (D^*\,EI_{eff}) \approx 13.75$

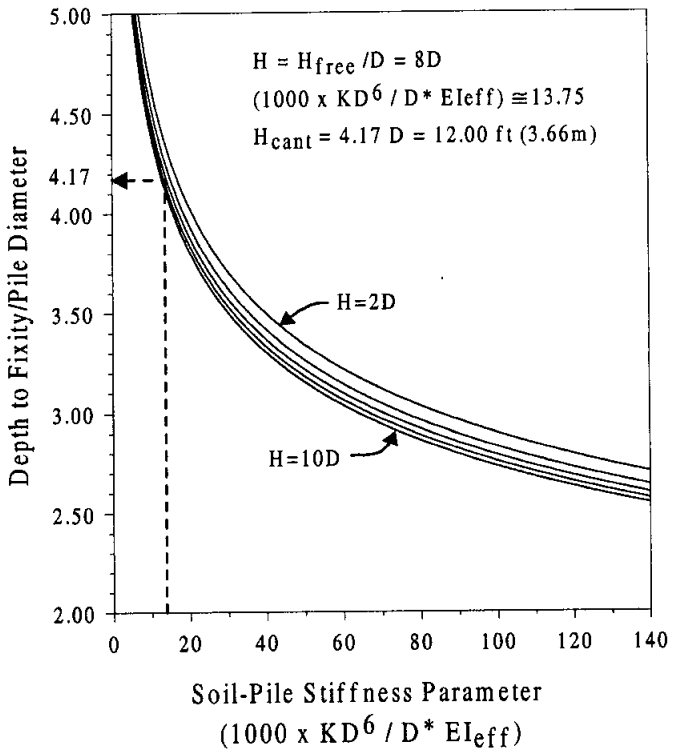

Figure 3-3 Effective Cantilever Length Calculations

The elastic period of the structure, T_N, was estimated at 1.07 sec, and calculations are presented in **Table 3-2**. As before, the distance from the cap beam center line to the center line of the superstructure center of mass was estimated at 7.00ft (2.13m).

The design moment calculations were then revised based on the effective cantilever length of 12.00ft (3.66m), the natural period of 1.07sec and the spectral acceleration of 0.69g. Calculations presented in **Table 3-3** indicate that the section, as described in **Figure 3-1(b)** and the corresponding moment curvature analysis presented in **Figure 3-2**, is adequate to resist the seismic moment of 17914 kips-in.(2023kN-m). The spectral acceleration was obtained from the design spectrum presented in **Figure 3-4**, which is the same outlined in **Chapter 2**.

Table 3-2 Natural Period - Rayleigh's Method

Member	W kips (kN)	K kips / ft (kN / m)	L ft (m)	ϕ i	$\Delta\phi$ i	W ϕ i^2	K $\Delta\phi$ i^2
Superstructure	2452 (10907)	1856 (27086)	19.0 (5.80)	1.00	0.44	2452 (10907)	359 (5244)
Column + Cap Beam	112 (498)	7360 (107411)	13.5 (4.11)	0.56	0.56	35 (156)	2308 (33684)
					Cantilevered Column, T = 1.07 sec	2487 (11063)	2667 (38928)

Table 3-3 Design Moment Calculations

Member	W kips (kN)	Cs g	V_E kips (kN)	V_D/Col kips (kN)	L ft (m)	M_D/Col kips-in. (kN-m)
Superstructure	2452 (10907)	0.69	1691.88 (7526)	105.75 (470)	13.5 (4.11)	17131.5 (1936)
Column + Cap Beam	112 (498)	0.69	77.28 (344)	4.83 (21.5)	13.5 (4.11)	782.5 (87)
				Design Moment for Individual Columns =		17914 (2023)

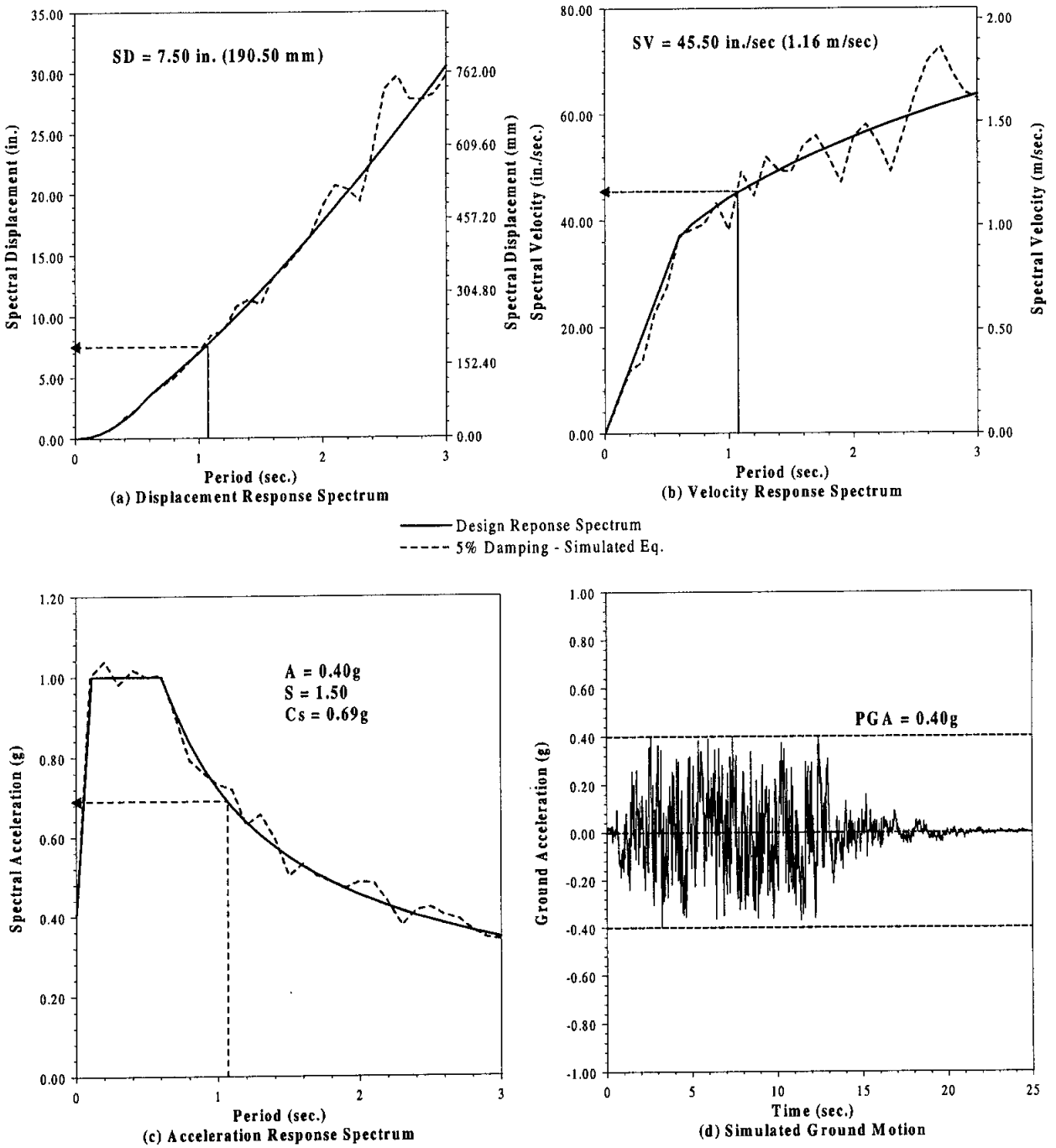

Figure 3-4 Simulated Ground Motion and Design Response Spectrum

3.2.1 Cap Beam Design

The design of the cap beam was performed considering the pile shaft/column overstrength, M^o_{col}, to ensure that the cap beam remains essentially elastic, and inelastic deformations are mainly concentrated in the column plastic hinges under the imposed gravity and seismic loads. Preliminary dimensions of the cap beam were computed based on the equations presented in **Table 3-4.**

Table 3-4 Cap Beam Design Dimensions

- Anchorage of Longitudinal Reinforcement
  $L_a \geq 0.025\ d_b\ \lambda_o\ f_y / \sqrt{f'_c} = 0.0025 \times 1.27 \times 1.40 \times 60000 / \sqrt{5000} = 37$ in. (940mm)
- Cap Beam Depth:
  $h_b = L_a + \text{Cover} + d_b \approx 35 + 5 = 40$ in. (Knik 36 in.)
- Cap Beam Width
  $W_b = D + 2 \times D/4 = 36 + 1.5 \times 36 = 54$ in. (Knik 54 in.)

Preliminary design forces for the cap beam flexural design were obtained based on the diagram presented in **Figure 3-4.** From geometry, preliminary bending moments for the design of the cap beam may be estimated as follows:

$$0.90\ M^d_{cap} = 1.05\ M^o_{col} \left(\frac{H_{cant}}{2/3\ L_b} \right) \left(\frac{2/3\ L_b - D/2}{H_{cant} - h_b/2} \right) \qquad (3.2)$$

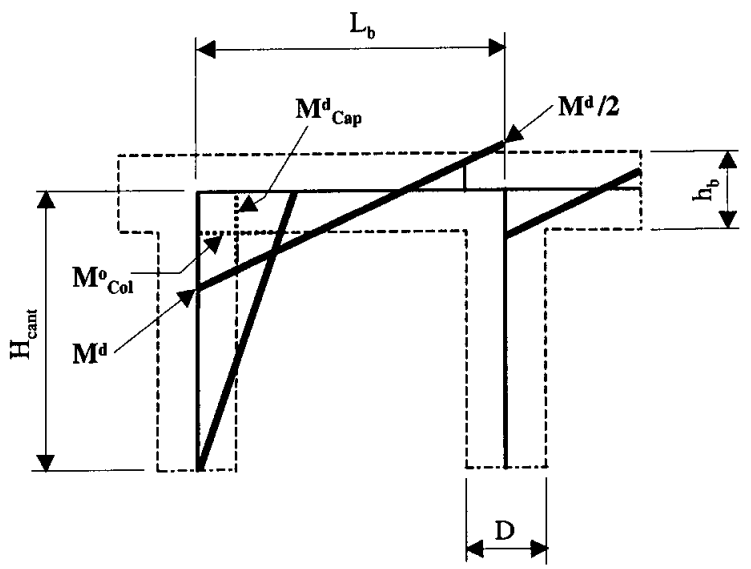

Given:

M^o_{col} = 21566kips-in.(2437kN-m) (per **Figure 3-2**)

H_{cant} = 12.00+1.5 = 13.50ft (4.11m)

L_b = 11.75ft (3.58m)

D = 36in. (914mm)

h_b = 42in. (1.07m) (per **Table 3-4**)

M^d_{cap} = 23372kips-in.(2641kN-m)

Figure 3-5 Cap Beam Preliminary Design Actions

Thus, the bending moment for the preliminary design of the cap beam longitudinal reinforcement was M^d_{cap} = 23372kips-in.(2641kN-m), as calculated in **Figure 3-5**. Moment curvature analysis presented in **Figure 3-6** indicates that the theoretical yield moment, which is 25300kips-in. (2859kN-m), is higher than the moment demand, thus the section presented in **Figure 3-7** was used in the pushover analysis to evaluate the seismic response of this preliminary design.

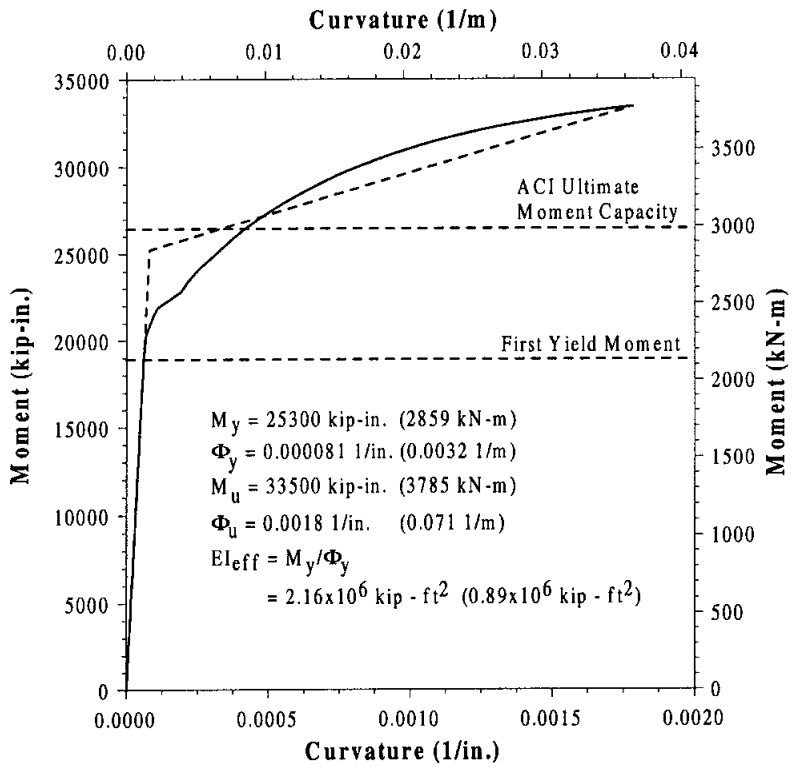

Longitudinal Reinforcement		Transverse Reinforcement	
Size	= #9	*Size*	= #4 (4-Legged)
Top Layer	= 8	*Spacing*	= 6.50in. (65.10mm)
Bottom Layer	= 8		
Side Layer	= 3		

Axial Load = -117kips (520kN)

Figure 3-6 Reinforced Concrete Section for the Cap Beam

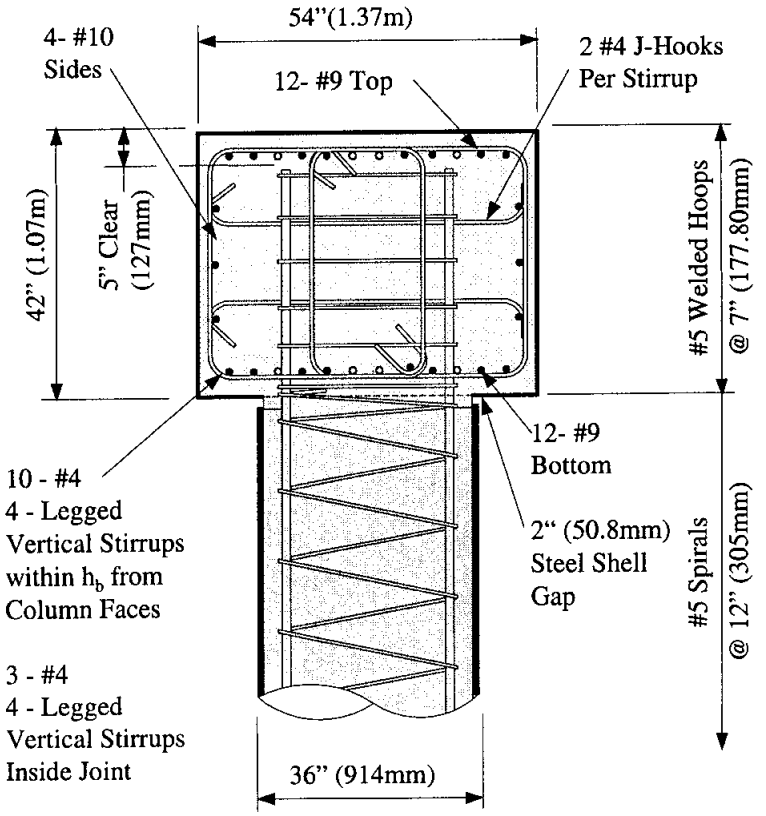

Figure 3-7 Column/Cap Beam Joint Section

3.2.2 Pushover Analysis Response and Design Calculations

In this section, a brief description of the pushover analysis response and calculations for the design of the cap beam are presented. The pushover analysis described in this section was performed according to the finite element model presented in **Chapter 2** and reference **[1]**. The column overstrength moments are largely dictated by the stress-strain characteristics of the longitudinal reinforcement. When the column longitudinal steel properties are available from material testing, Sritharan et al.**[4]** recommend that the column overstrength moment be approximated to 1.05 times the *theoretical maximum moment*. The cap beam design bending moments presented in **Figure 3-8** were estimated according to the expressions:

$$\varphi_f M_{D,cap} = 1.05\ M_E + M_D \qquad (3.3)$$

Where φ_f is equal to 0.90 and represents the flexural capacity strength reduction factor and $M_{D,cap}$ is the cap beam design moment calculated at the column face, as described in **Figure 3-8**. In

addition, M_E is the bending moment caused by lateral forces, which is obtained by subtracting M_D from M_{E+D}. Bending moments that result from gravity loads, M_D, alone are presented in **Figure 3-9**, and bending moments that result from gravity loads plus lateral forces, M_{E+D}, are presented in **Figure 3-10**.

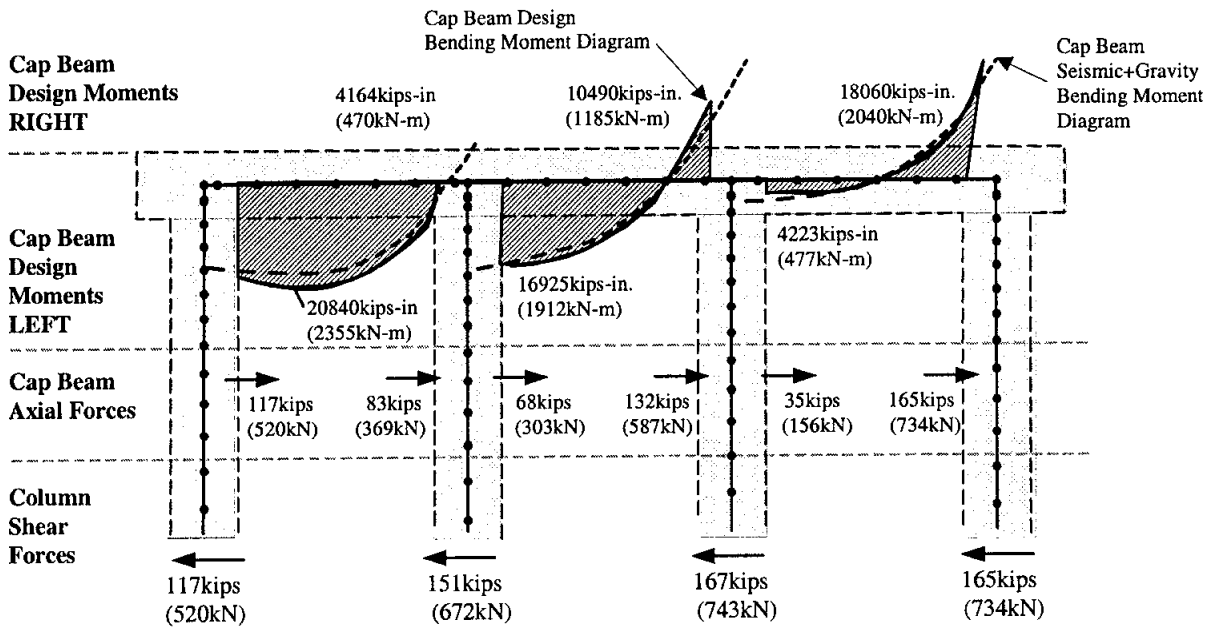

Figure 3-8 Cap Beam Design Moments

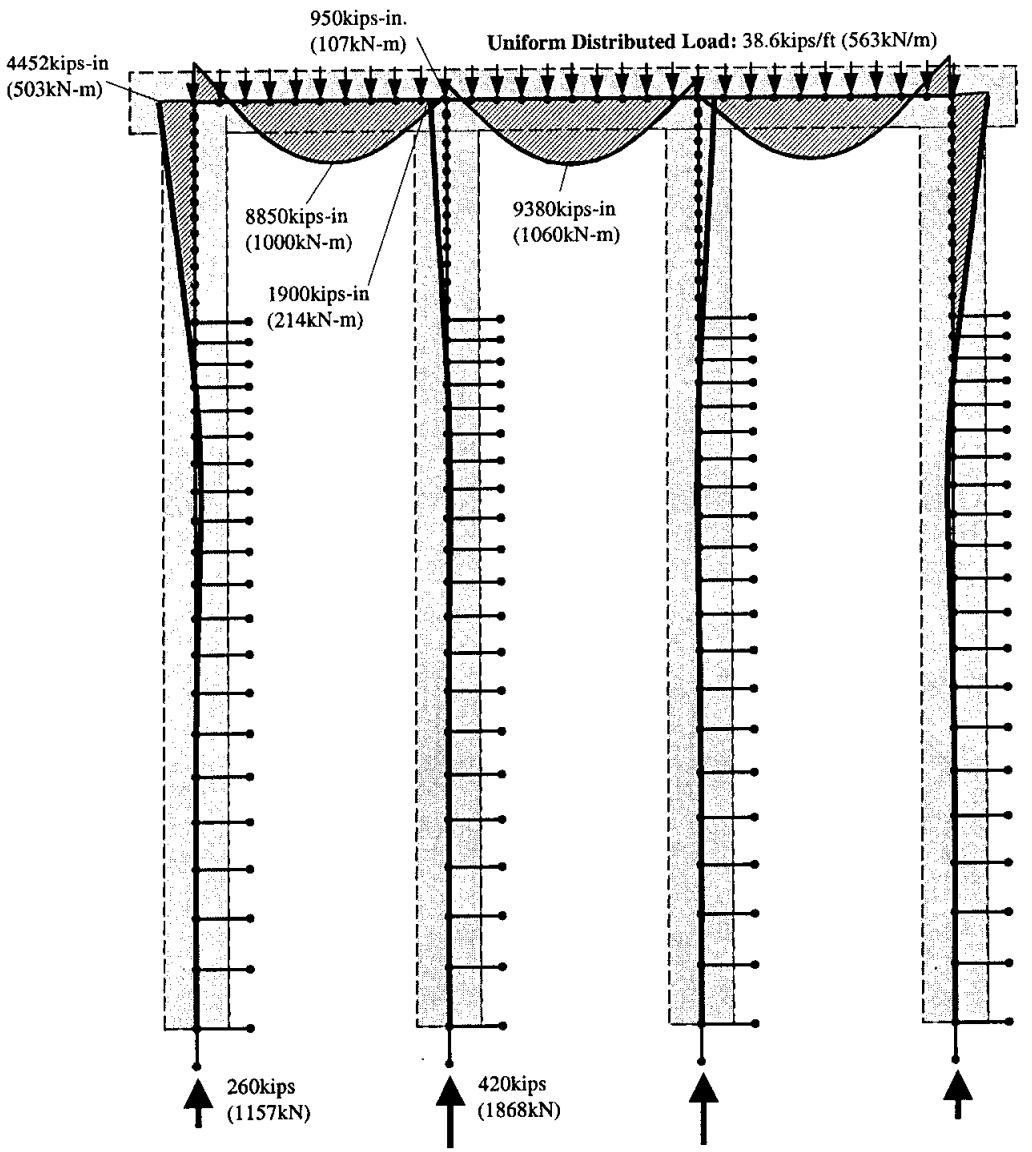

Figure 3-9 Gravity Loads Bending Moment Diagram

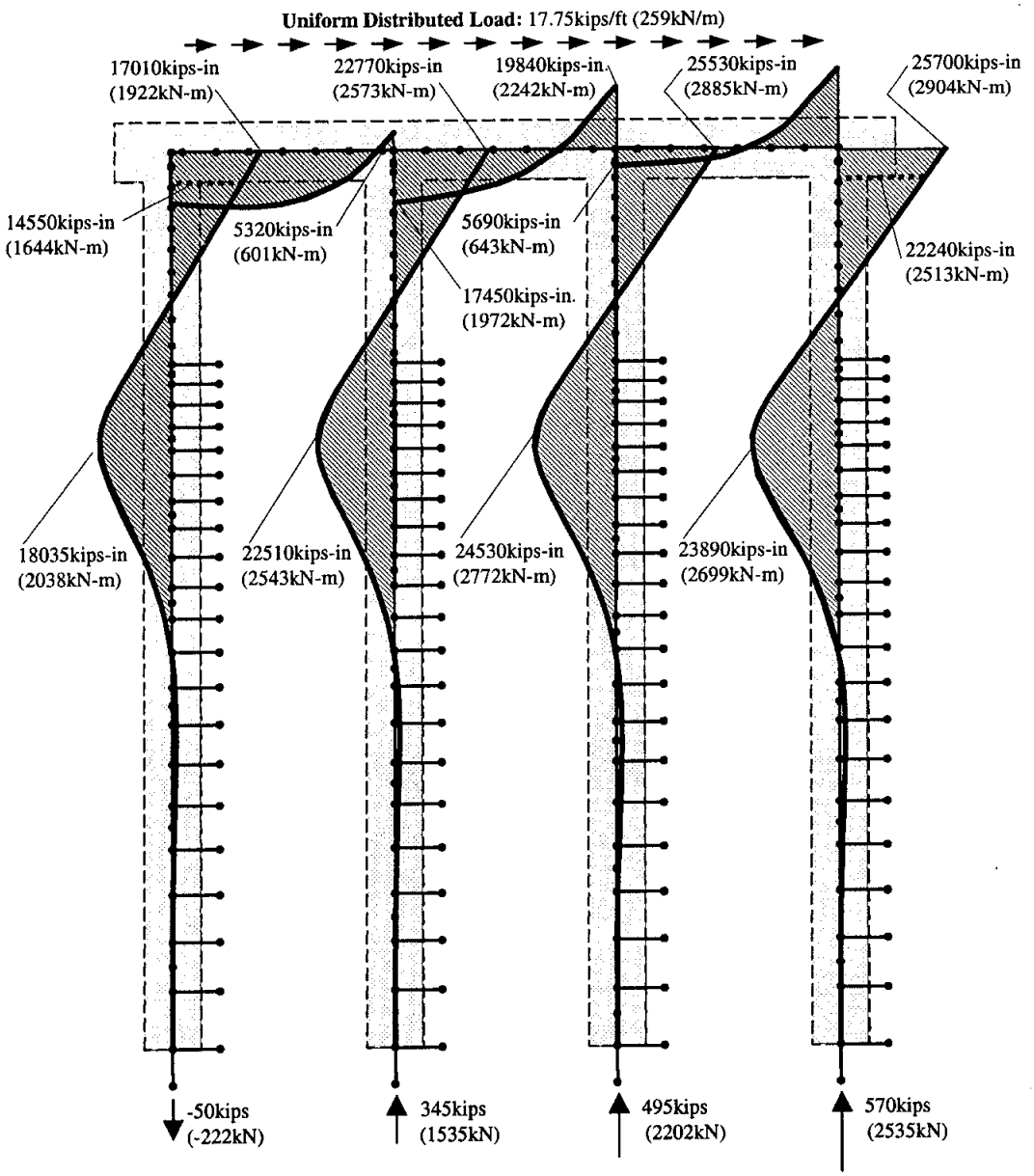

Figure 3-10 Gravity + Seismic Loads Bending Moment Diagram

Similar to the design moments, design shear forces were computed at the column faces according to the expression :

$$\varphi_s V_{D,cap} = 1.05 V_E + V_D \quad (3.4)$$

where φ_s is equal to 0.85 and represents the capacity reduction factor for shear, and $V_{D,cap}$ is the design shear force evaluated at the column face, as presented in **Figure 3-11**. In addition, V_E is the shear force caused by lateral forces, which is obtained by subtracting V_D from V_{E+D}. Shear forces that result from gravity loads, V_D, alone are presented in **Figure 3-12**, and shear forces that result from gravity loads plus lateral forces, V_{E+D}, are presented in **Figure 3-13**.

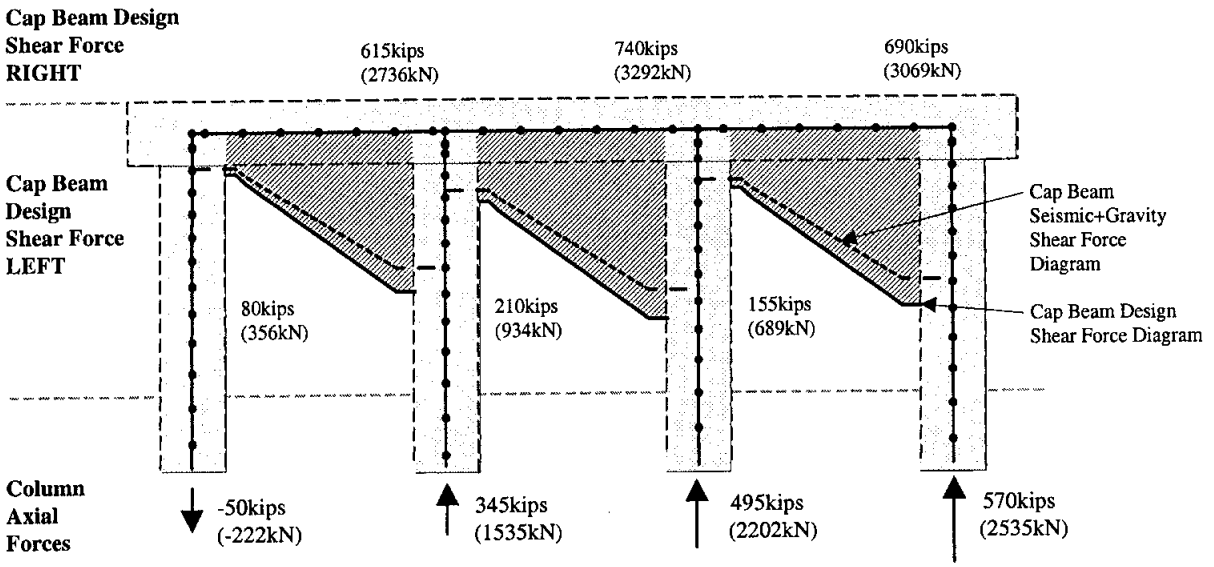

Figure 3-11 Cap Beam Design Shear Forces

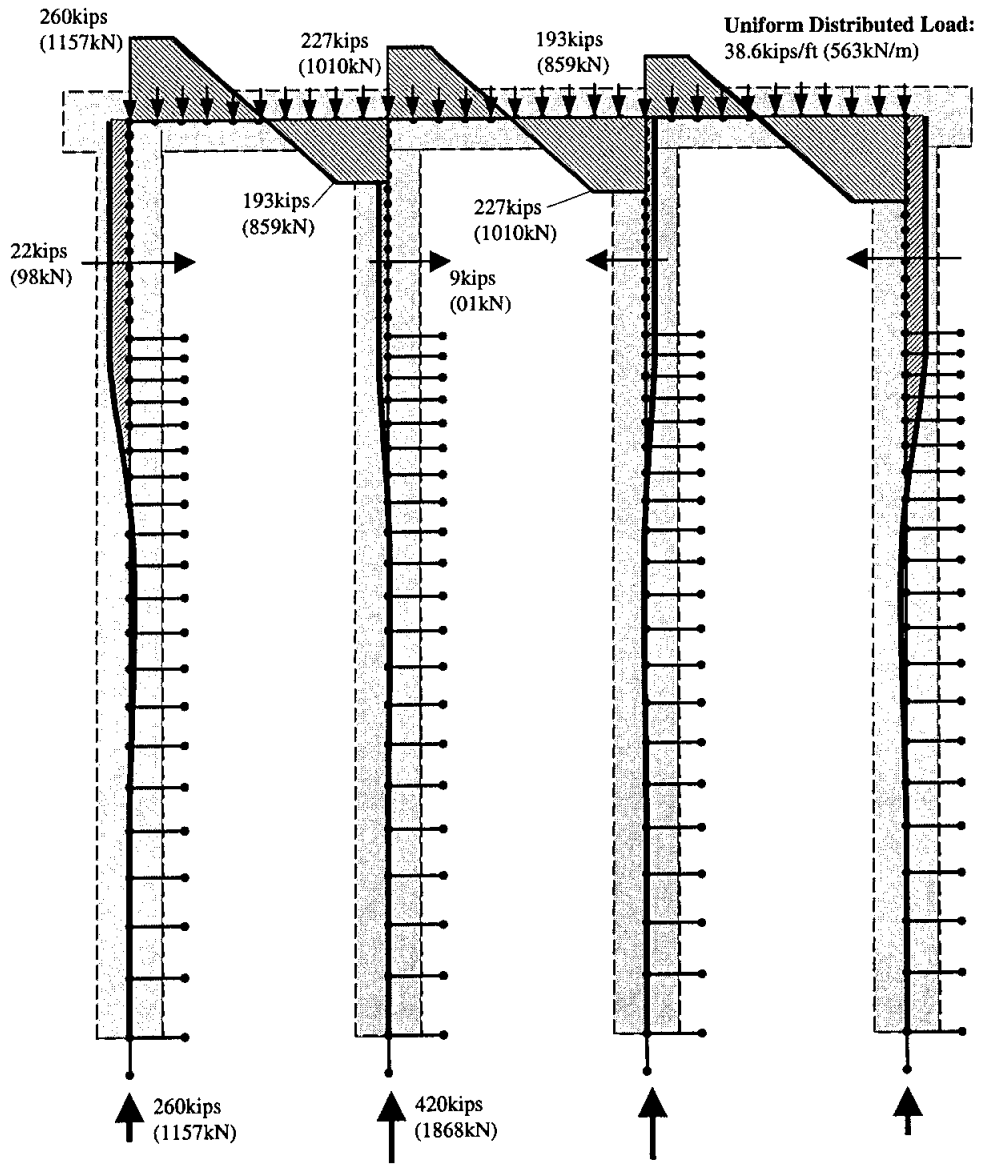

Figure 3-12 Gravity Loads Shear Force Diagram

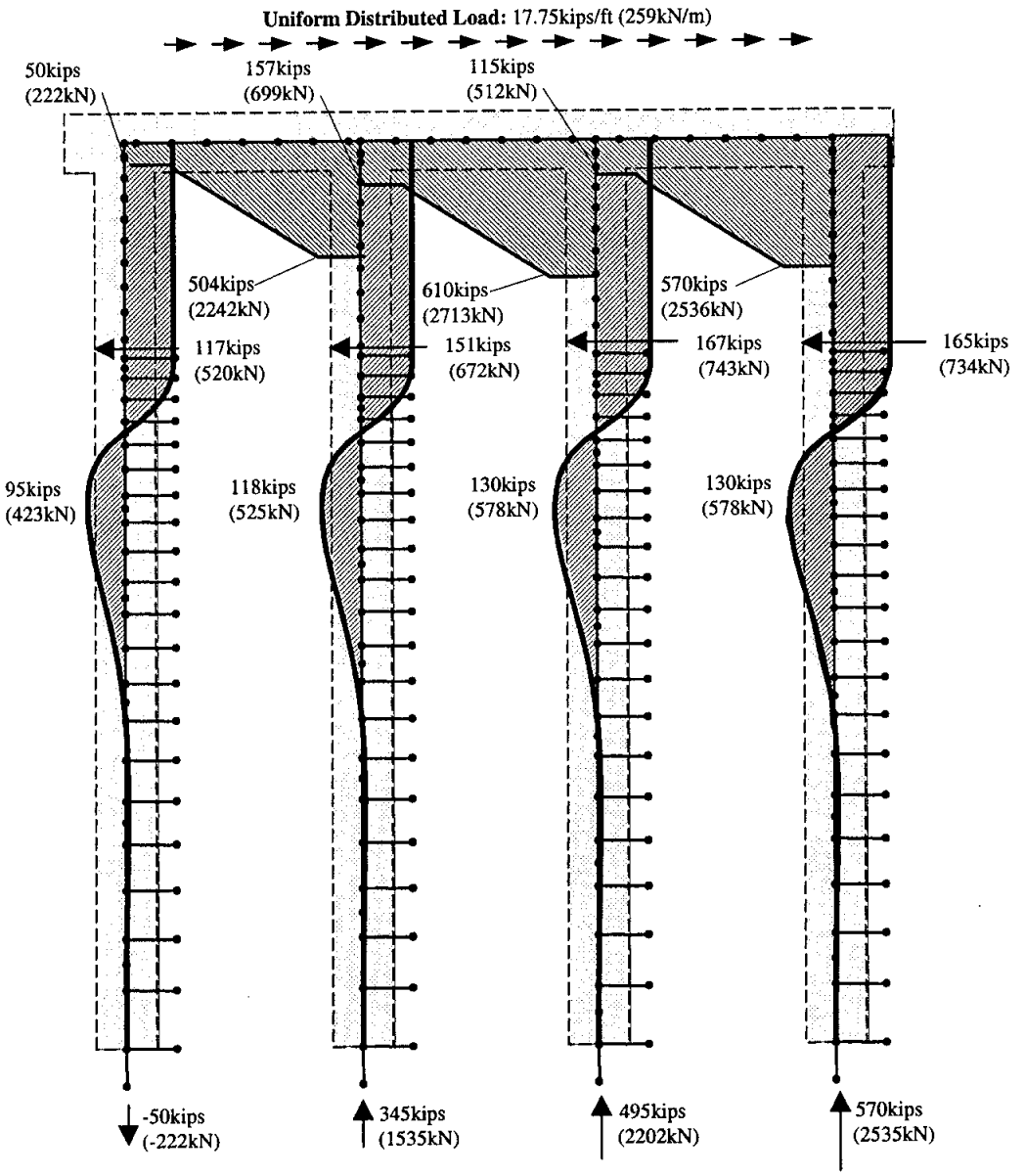

Figure 3-13 Gravity + Seismic Loads Shear Force Diagram

According to a capacity design philosophy it is required that undesirable modes of deformation such as shear be inhibited, and the columns must be designed with adequate transverse reinforcement to ensure adequate confinement of the column plastic hinges. In addition, design of the cap beam was performed considering the column overstrength, to ensure that the cap beam remains essentially elastic and inelastic deformations are concentrated in the column plastic hinges under the imposed gravity and seismic loads. The column overstrength moment consider material uncertainties and strain hardening of the column longitudinal reinforcement. Design of the cap beam was based on the design procedure outlined in reference **[1]** and calculations are presented in **Tables 3-5** through **3-7.**

Table 3-5 Cap Beam Reinforcement Design

- Design Moments
  $\phi_f M_{CAP} = 1.05 M_E + 1.00 M_D$, $\phi_f = 0.90$
  (See **Figure 3-8** for Cap Beam Design Moment Diagram Diagram)

- Design Shear
  $\phi_s V_{CAP} = 1.05 V_E + 1.00 V_D$, $\phi_s = 0.85$
  (See **Figure 3-11** for Cap Beam Shear Force Design Diagram)

- Cap Beam Shear Design ASCE-ACI 426:
  $v_b = (0.80 + 120 \rho_{bt}) \sqrt{f_c'} =$
  $(0.80 + 120 \times 0.0036) \sqrt{3000} = 68$ psi $< 2.4 \sqrt{f_c'}$ psi $(0.2 \sqrt{f_c'}$ MPa)

  $v_c = v_b \times (1 + 3 P / (f_c' A_g)) =$
  $68 \times (1 + 3 \times 132000 / (3000 \times 54 \times 42) = 72$ psi
  (Interior Column is Critical see **Figure**)

  $V_c = 0.80 v_c \times A_g = 131$kips (581kN)

  $s = A_{sp} f_y h_b \cot \theta / (V_{des} - V_c) = 4 \times 0.20 \times 60 \times 40 \times \cot 35 / (740 - 131)$
  ≈ 6.50in. (165.10mm)
  $s_{max} \leq h_b / 4 \leq 10.50$in. (267mm) **Use #4 at 6.50 in o/c** (4 legged stirrups)

Table 3-6 Principal Stress Calculations

(Trailing Column):

- *Joint Shear Stress*
  $v_{jh} = M_c^o / (h_b \sqrt{2D^2}) = 20840 / (42 \times 1.41 \times 36^2) = 270\text{psi}$ (1.87MPa)
- *Vertical Axial Stress*
  $f_v = P_c / ((h_b + D) \sqrt{2D}) = -50 / ((42 + 36) \times 1.41 \times 36) = -13\text{psi}$ (0.09MPa)
- *Horizontal Axial Stresses*
  $f_h = V_b / (h_b \times w_b) = -117 / (42 \times 54) = -52\text{psi}$ (0.36MPa)
- *Principal Tension Stress*
  $p_t = (f_v + f_h)/2 - \sqrt{(f_v - f_h)^2/ 4 + v_{jh}^2} = -303\text{psi}$ (2.09MPa) $\approx 5.53 \sqrt{f_c'} > 5.00 \sqrt{f_c'}$
- *Principal Compression Stress*
  $p_c = (f_v + f_h)/2 + \sqrt{(f_v - f_h)^2/ 4 + v_{jh}^2} = +238\text{psi}$ (1.64MPa) $\approx 0.08 f_c' < 0.30 f_c'$

(Leading Column):

- *Joint Shear Stress*
  $v_{jh} = M_c^o / (h_b \sqrt{2D^2}) = 18060 / (42 \times 1.41 \times 36^2) = 235\text{psi}$ (1.62MPa)
- *Vertical Axial Stress*
  $f_v = P_c / ((h_b + D) \sqrt{2D}) = 570 / ((42 + 36) 1.41 \times 36) = 144\text{psi}$ (1.00MPa)
- *Horizontal Axial Stresses*
  $f_h = V_b / (h_b \times w_b) = 165 / (42 \times 54) = 73\text{psi}$ (0.50MPa)
- *Principal Tension Stress*
  $p_t = (f_v + f_h)/2 - \sqrt{(f_v - f_h)^2/ 4 + v_{jh}^2} = -130\text{psi}$ (0.90MPa) $\approx 2.40 \sqrt{f_c'} < 5.00 \sqrt{f_c'}$
- *Principal Compression Stress*
  $p_c = (f_v + f_h)/2 + \sqrt{(f_v - f_h)^2/ 4 + v_{jh}^2} = +346\text{psi}$ (2.39MPa) $\approx 0.12 f_c' < 0.30 f_c'$

Based on Principal Tension Stress :

Design Joint with Maximum Required Joint Shear Reinforcement

Based on Principal Compression Stress :

Section is okay to Prevent Crushing of Concrete in the Joint Region

Table 3-7 Joint Shear Reinforcement

- External Joint Vertical Stirrups

  $A_{jv} = 0.125 \times 1.40 \times 12 \times 1.27 = 2.67 in.^2$ ($1721 mm^2$)

  Use 4 - #4 (4 legged stirrups)

  within 40in. From column face

- Internal Joint Vertical Stirrups

  $A_{jv} = 0.095 \times 1.40 \times 12 \times 1.27 = 2.03 in.^2$ ($1308 mm^2$)

  Use 3 - #4 (4 legged stirrups)

  Inside Joint Region

- Additional Cap Beam Top Layer

$\Delta A_{tb} = 0.17 \times 1.4 \times 12 \times 1.27 = 3.63 in.^2$ **Use 4 - #9**

- Additional Cap Beam Bottom Layer

$\Delta A_{tb} = 0.15 \times 1.4 \times 12 \times 1.27 = 3.20 in.^2$ **Use 4 - #9**

- Joint Horizontal Hoops

$\rho_s = 0.30 \times \lambda_o \times A_{sc} f_{yc} / (f_{yv} L_a^2) = 0.30 \times 1.4 \times 15.24 / 35^2 = 0.53\%$

$\rho_s \geq 3.50 \sqrt{f_c'} / f_{yh} = 3.50 \sqrt{3000} / 60000 = 0.32\%$

$s = 4 A_{sh} / D' \rho_s = 4 \times 0.31 / (36 - 4) \times 0.0053 = 7.30 in.$ (185.70mm)

Use #5 at 7 in. o/c

The pushover analysis lateral force-deformation relationships and limit states for the redesigned bridge bent are plotted in **Figure 3-14**. Limit states presented in **Figure 3-14** indicate that full formation of the plastic mechanism in the gap region will be ensured due to additional capacity of the cap beam from shear and flexural considerations. In addition, failure of the joint regions will not occur because of the additional reinforcement provided in the joints.

Presented in **Figure 3-14** are the spectral forces and displacement obtained from the time history, which will be presented in the next section. According to the spectral displacement the structure has reserved displacement ductility capacity to withstand the imposed displacement of 8in. (203.20mm). Thus, with proper detailing of the cap beam, full formation of the plastic mechanism in the gap region will be ensured.

Cap beam and column moment curvature relationships are presented in **Figure 3-15**. Unlike results described in **Chapter 2**, columns will be subjected to higher curvature ductility demands than the in cap beams, as expected from capacity design principles.

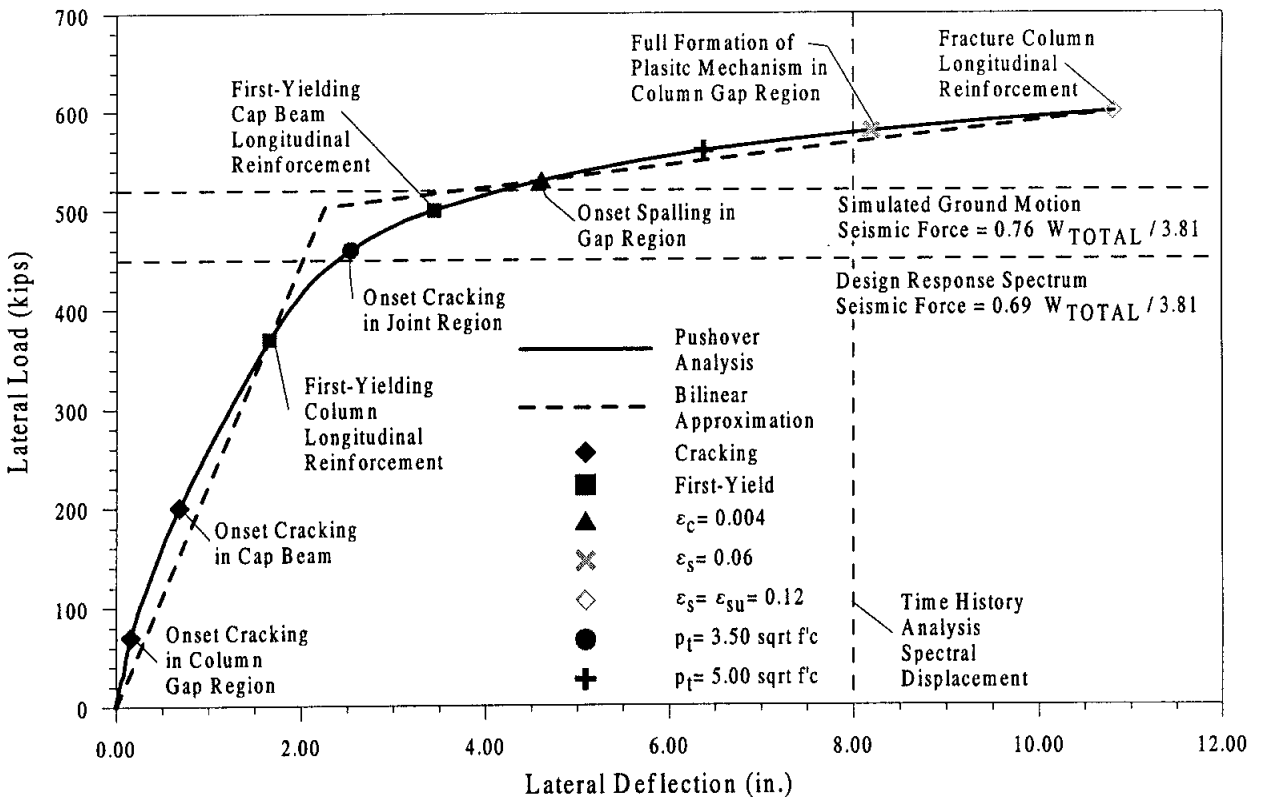

Figure 3-14 Lateral Force-Deformation and Limit States From Pushover Analysis

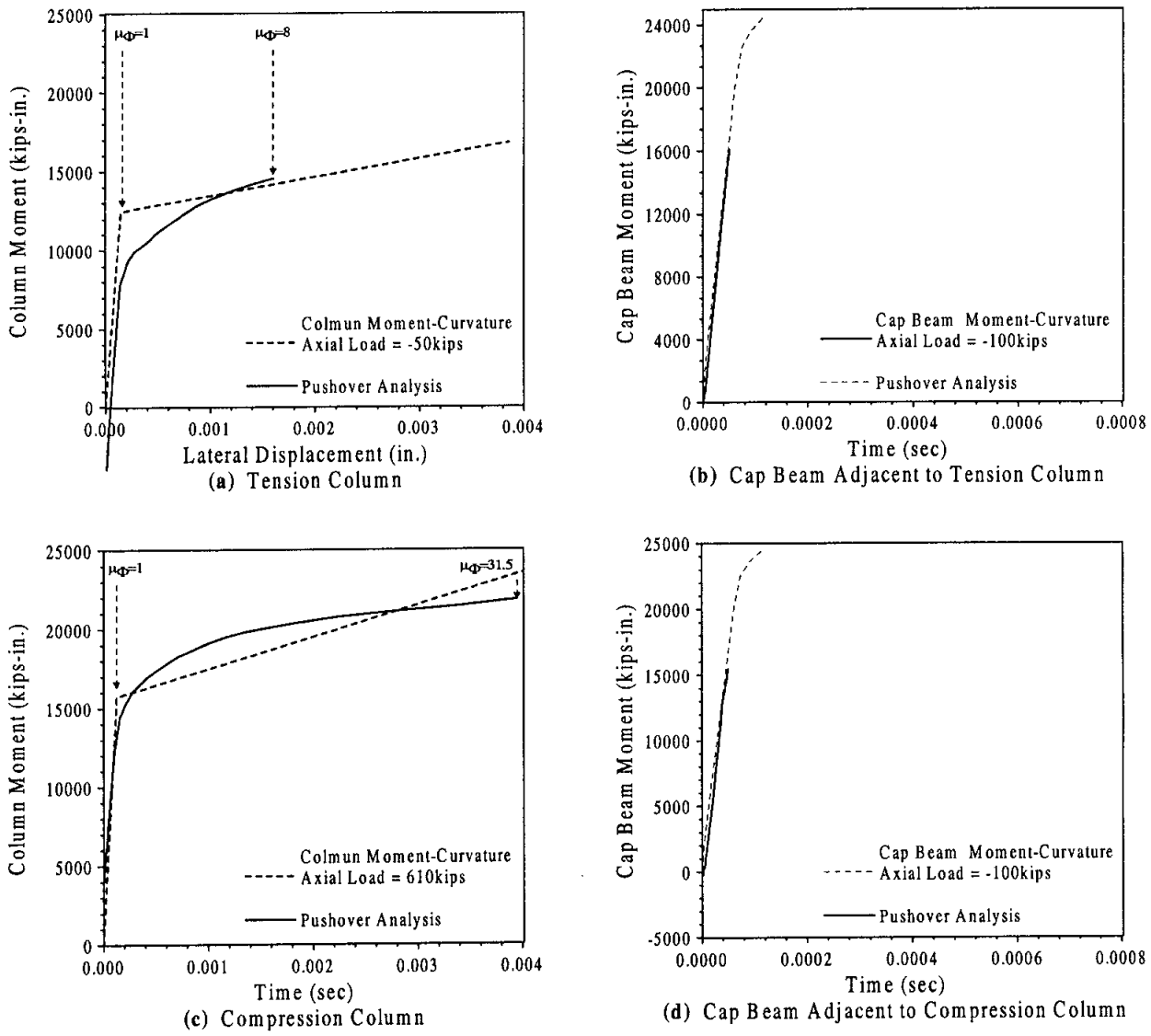

Figure 3-15 Pile Shafts/Columns and Cap Beam Moment-Curvature Relationships From Pushover Analysis

3.3 Time History Analysis Response

Similar to the procedure outlined in **Chapter 2**, an elastic and nonlinear time history analyses were performed using the simulated ground motion presented in **Figure 3-4(d)**, and the finite element model described in **Chapter 2**. The modified Takeda model was the model used to characterize the hysteretic behavior of the columns and cap beam. This model was based on the bilinear approximation presented in **Figures 3-2** and **3-6** for the columns and cap beam, respectively.

Elastic and nonlinear moments at top the columns located on the extreme sides and adjacent cap beam moments are plotted in **Figures 3-16(a)** and **3-16(b)**, respectively. Calculations for force reduction factors are presented in **Table 3-8**, which indicate that a force reduction factor, R, of approximately 3.81 will be achieved, which is approximately the design force reduction factor of **4**. In addition in **Figures 3-16(c)** and **3-16(d)** are presented the column top displacement for the elastic and nonlinear analysis, respectively. Values presented in **Table 3-6** indicate that a displacement ductility, μ_Δ, of approximately 3.96 will be achieved, which is slightly smaller than the design displacement ductility of **4**. This value is approximately the same as the R value, which characterizes the equal-displacement principle established for an inelastic system [2]. These values indicate that the seismic response of the redesigned bridge bent is within the design requirements.

In **Figure 3-17(a)** and **3-17(b)** are presented the columns and cap beam moment-curvature relationships, respectively, obtained from the nonlinear time history analysis. Referring to **Figure 3-17(a)**, it is clear that the columns under the imposed seismic actions will be subjected to increased inelastic deformations than in the cap beam, as illustrated in **Figure 2-17(b)**. Thus, the cap beam design is adequate to ensure proper formation of the plastic hinges in the columns gap region at the cap beam interface.

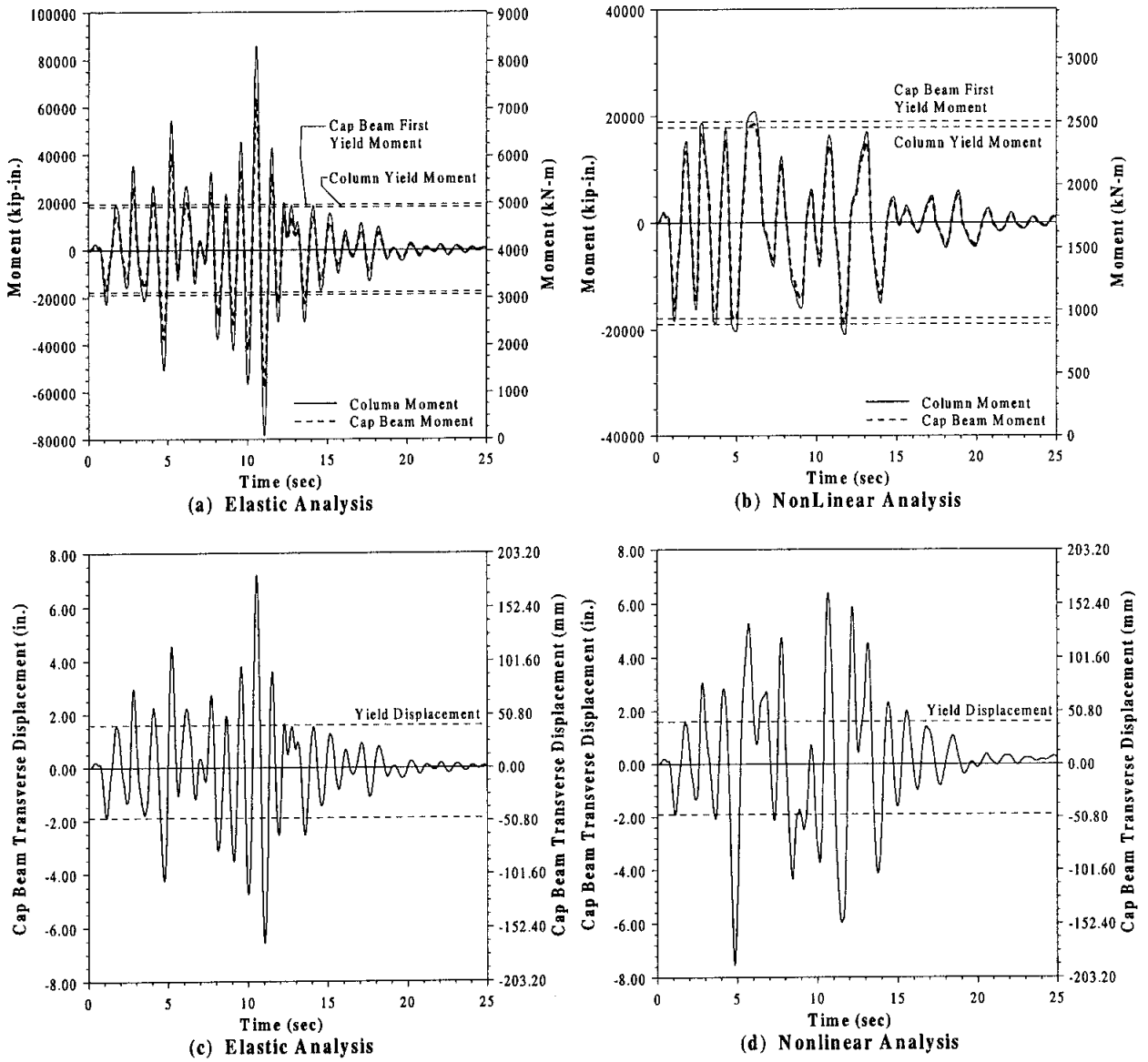

Figure 3-16 Simulated Ground Motion Time History Linear and Nonlinear Analysis

Table 3-8 Force Reduction Calculations
From Time History Analysis

	W_{TOTAL} kips (kN)	V_E kips (kN)	Cs g	V_D kips (kN)	R V_E / V_D
Bridge Weight	2600 (11565)	1980 (8807)	0.76	520 (2313)	3.81

Table 3-9 Displacement Ductility Calculations
From Time History Analysis

	Δ_y in. (mm)	Δ_d in. (mm)	$\mu\Delta_d$
Column Top Displacement	1.90 (48.26)	7.53 (191.26)	3.96

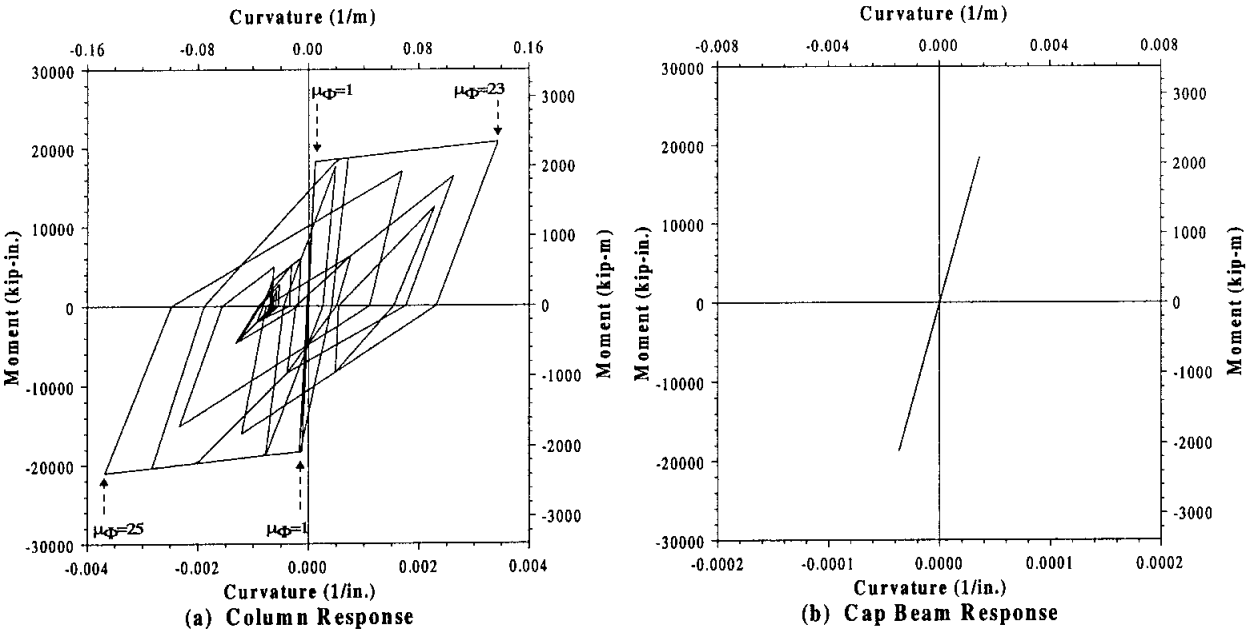

Figure 3-17 Moment vs. Curvature Time History Nonlinear Analysis

4 CONCLUSIONS

Redesign of the Knik River Overflow Bridge is presented in this report. Redesign of this bridge bent was performed using the multiple column bridge bent design recommendations presented in the full-scale proof test of a bridge bent having three cast-in-place steel shell columns report [1], which was prepared for the Alaska Department of Transportation and Public Facilities.

In the redesign of the bridge bent, the plastic hinges were selected at the top of the columns and the cap beam was designed to remain essentially elastic according to the capacity design philosophy. Redesign of the cap beam was performed in accordance with the capacity design philosophy utilizing research findings from previous studies at UCSD [1]. The cap beam width was related to the column diameter by **1.5D**, which is consistent with current seismic design practice. When designing the column/cap beam joints, emphasis was placed in minimizing reinforcement quantities so that constructable joint details are obtained. Anchorage of the column longitudinal reinforcement into the cap beam was achieved with straight bar ends since J-hooks or tails at bar ends can also create congestion of reinforcement in the joint zones. In addition, the steel shells were terminated below the cap beam to avoid premature damage in the beam by the steel shell during lateral load response.

Pushover and time history linear and nonlinear analyses were performed according to the models described in **Chapter 3**. The analytical results indicate that the redesign is sufficient in ensuring that plastic hinges will form at the top of the pile shaft/columns in the gap region.

Based on the design and performance of the multi-column bent test unit and other recently completed UCSD research studies, a detailed list of design recommendations are presented in reference [1] for the seismic design of multi-column bridge bents with circular CISS-columns. It is assumed that multi-column bridge bents are designed using the capacity design philosophy with hinges forming at the column ends. Redesign of the Knik River Overflow Bridge was based on the these list of design recommendations, and it is ensured that a ductile seismic response can be expected up to the design drift limit state.

References

[1] Silva, P. F., Sritharan, S., Seible, F., Priestley, M. J. N., "A *Full-Scale Proof Test of the Alaska Cast-in-Place Steel Shell Three Column Bridge Bent Test,"* Report # SSRP-98/13, Department of AMES , University of California, San Diego, La Jolla, California, February 1999.

[2] Priestley, M. J. N., Seible, F., Calvi, M., *" Seismic Design and Retrofit of Bridges, "* John Wiley & Sons, Inc. , New York, September 1995, 672 pages.

[3] Silva, P. F., Seible, F., Priestley, M. J. N., *"Response of Standard Caltrans Pile-to-Pile Cap Connections Under Simulated Seismic Loads"*, Department of AMES , University of California San Diego, La Jolla, California, November 1997, Report # SSRP-97/09.

[4] American Association of State Highway and Transportation, *Standard Specifications for Highway Bridges"* 7th Edition, 1996.